

# Prepared discussion

Objekttyp: **Group**

Zeitschrift: **IABSE reports of the working commissions = Rapports des commissions de travail AIPC = IVBH Berichte der Arbeitskommissionen**

Band (Jahr): **4 (1969)**

PDF erstellt am: **22.05.2024**

## **Nutzungsbedingungen**

Die ETH-Bibliothek ist Anbieterin der digitalisierten Zeitschriften. Sie besitzt keine Urheberrechte an den Inhalten der Zeitschriften. Die Rechte liegen in der Regel bei den Herausgebern.

Die auf der Plattform e-periodica veröffentlichten Dokumente stehen für nicht-kommerzielle Zwecke in Lehre und Forschung sowie für die private Nutzung frei zur Verfügung. Einzelne Dateien oder Ausdrucke aus diesem Angebot können zusammen mit diesen Nutzungsbedingungen und den korrekten Herkunftsbezeichnungen weitergegeben werden.

Das Veröffentlichen von Bildern in Print- und Online-Publikationen ist nur mit vorheriger Genehmigung der Rechteinhaber erlaubt. Die systematische Speicherung von Teilen des elektronischen Angebots auf anderen Servern bedarf ebenfalls des schriftlichen Einverständnisses der Rechteinhaber.

## **Haftungsausschluss**

Alle Angaben erfolgen ohne Gewähr für Vollständigkeit oder Richtigkeit. Es wird keine Haftung übernommen für Schäden durch die Verwendung von Informationen aus diesem Online-Angebot oder durch das Fehlen von Informationen. Dies gilt auch für Inhalte Dritter, die über dieses Angebot zugänglich sind.

## DISCUSSION PRÉPARÉE / VORBEREITETE DISKUSSION / PREPARED DISCUSSION

**Prediction of Behavior of Steel Columns Under Load**

Le comportement des poteaux en acier soumis à la compression

Das Verhalten von belasteten Stahlstützen

LAMBERT TALL      GÖRAN A. ALPSTEN  
U.S.A.                      Sweden

INTRODUCTION

The prediction of the behavior of compression members under load depends on a knowledge of material properties and geometry. There may be considerable scatter in both--in particular, residual stresses and out-of-straightness are predominant factors. Residual stresses are the initial stresses existing in a member before the application of external load. Out-of-straightness is used here to refer to all deviations which result in an eccentrically loaded column, that is, initial curvature, eccentric application of load, and unsymmetrical residual stress distribution.

This paper summarizes some aspects of a continuing general study of the stability of plates and columns underway at Lehigh University for the past two decades. The initial work, concerned mainly with small to medium-size rolled steel shapes, formed the basis for design recommendations subsequently incorporated into the U.S. specifications. Later investigations have included welded column shapes also. Current column research at Lehigh University deals with welded shapes built up from flame-cut plates and with very heavy shapes, rolled as well as welded members, of sizes up to 1122lb/ft.

Although studies at Lehigh University have considered simple columns, beam-columns, and framed columns, this paper includes only the simple columns, since a large number of variables have been considered in its study, and since it is, essentially, the basic column, to which the strength of other columns may be referred.

BASIC COLUMN STRENGTH

The strength of a simple column may be typified by its maximum (or ultimate) load. For any particular column cross section and material, the maximum load depends both on the magnitude and distribution of residual stresses within the cross section, and on the initial out-of-straightness. For the hypothetical case of zero initial out-of-straightness, the column remains straight under increasing load until the tangent modulus load is reached. The level of the tangent modulus load is greatly affected by the residual stresses. At the tangent modulus load, the column bifurcates and then continues deflecting under increasing load, reaching the maximum load, after which it starts unloading. See Fig. 1.

While laboratory testing techniques may simulate closely the behavior of a perfectly straight column (See Fig. 2), practical columns show an initial out-of-straightness which will cause the column to deflect immediately upon

loading. The deflection will increase gradually under increasing load up to the maximum load, as shown in Fig. 1. The maximum load of the column with initial out-of-straightness is reduced as compared to the perfectly straight column with other conditions the same. The maximum load and the shape of the load-deflection curve are affected by residual stresses and out-of-straightness. The unloading characteristics may be important when considering the framed column member in a structure--it is normally desirable that the column can sustain loads at or close to the maximum for relatively large deflections.

#### EFFECT OF VARIATIONS IN RESIDUAL STRESSES AND OUT-OF-STRAIGHTNESS

As noted above, the mechanical and geometrical properties of the column, including in particular residual stresses existing in the member and initial out-of-straightness, are of the utmost importance in their effect on column strength. These properties can vary considerably between different members, as well as between different elements of same fabrication conditions and cross-sectional geometry, and also within the member itself. This variation or scatter has been studied extensively, and some results of the variation in yield strength and residual stresses have been summarized in Ref. 1.

The formation of residual stresses is dependent on the manufacturing and fabrication processes used, as well as on the size and geometry of a particular member. [2] Thus, it may be expected that the fabrication and geometry are important factors in determining the strength of steel columns. The variations in manufacturing and fabrication processes, and in the member size and geometry, all lead to a scatter in the residual stresses, which when combined with the variation of material properties, will lead to a scatter in column strength both in the behavior under load, and in the maximum load. Similarly, the out-of-straightness characteristics are a result of the manufacture and fabrication which will introduce scatter in column strength. Indeed, a summary of all column test results obtained shows a tremendous variation, even when compared on the basis of equal yield strength as shown in Fig. 3. It should be noted that the testing method used for most of the column tests included in Fig. 3 involves a special alignment procedure, [3] designed so that the effect of out-of-straightness is minimized. Thus, it may be expected that the consideration of full variations in out-of-straightness would lead to additional scatter in the column test results of Fig. 3.

Most of the variation in column results, however, can be attributed to predictable variations in the residual stresses or other factors such as out-of-straightness, which could be controlled in the design or fabrication process. The strength of columns, and the consideration of the scatter in material properties, may be considered in either of two basic ways: (1) a statistical study of strength irrespective of causes, or (2) a theoretical study of mathematical models where all the variables may be considered either independently or together. The former is experimental, and the latter is theoretical with experimental correlation.

The Lehigh University studies of column strength have followed the second consideration--typical and possible variations in the influencing factors were considered and it was investigated theoretically whether these made significant variations in structural behavior. The verifying experiments were deterministic, rather than probabilistic, in nature. This approach was chosen

mainly for reasons of economy and time, and for the fact that the influence of each variable could be considered separately in order to understand fundamental behavior. The variables considered were residual stress, out-of-straightness, yield strength, manufacturing and fabrication processes (for instance, hot-rolled or welded) and details (for instance, weld method and heat input), and size and geometry of the cross section. The mathematical models used considered the simultaneous elastic and plastic regions at all stages during the loading process. Some effects, such as residual stresses, predominate in these column studies, and efforts were made to find ways of changing the residual stress distribution into a more favorable one. It is not believed that purely statistical studies would lead to methods of improving strength.

### PREDICTION OF COLUMN STRENGTH

Two methods for the forecasting of the structural behavior of a simple column will be considered here. These methods are based upon the tangent modulus load concept ("T.M. prediction") and the maximum load of the column ("M.S. prediction"), respectively. The tangent modulus prediction, as generalized to include the effect of residual stresses, [4,5], considers a fictitious, perfectly-straight column with centric load application and symmetrical residual stresses. (See also Fig. 1.) It may be shown that the tangent modulus prediction under certain assumptions applicable to members of structural carbon steel is a function of the moment of inertia of the elastic part of the cross section, [5] or

$$\frac{P_{TM}}{A} = \frac{\pi^2 E I_e}{(L/r)^2 I} \quad (1)$$

where  $P_{TM}$  is the tangent modulus load,  $A$  is the cross-sectional area,  $E$  is the elastic modulus,  $I_e$  is the moment of inertia of the elastic part of the cross section,  $I$  is the total moment of inertia about the axis considered,  $L$  is the effective length of the column, and  $r$  is the radius of gyration of the cross section. The extension of the elastic areas of the cross section is dependent on the residual stresses and the applied strain. Typical column curves from tangent modulus predictions are shown in Fig. 4. ( $P_{cr}$  is the critical load, in this case the tangent modulus load.)

The maximum strength prediction is somewhat more complex to calculate. The basic concepts, however, are very simple--the theory is based upon equilibrium conditions for the deflected position of the column. The theory may be applied to the prediction of the post-buckling strength of the initially straight centrally loaded column as well as to the more practical case with initial out-of-straightness. The maximum load marks the position where, under increasing deflection, the rate of the resisting internal moment in the column is equal to the rate of the externally applied moment. Several studies have considered methods to calculate the maximum load, including the effect of residual stresses and initial-out-straightness. [6 through 11] An example of a maximum strength curve is given in Fig. 5, and compared with the corresponding tangent modulus curve. [12] In this particular case, the maximum strength



curve, based upon predicted residual stresses in a hot-rolled 14WF730 "jumbo" shape with an initial deflected curve of  $\delta_{\max}/L=0.001$ , falls slightly below the tangent modulus curve.

For a general investigation of the column strength as affected by accurate residual stress distributions and out-of-straightness, the numerical computations will become quite cumbersome and tedious, necessitating the use of an electronic computer. General programs have been developed for tangent modulus as well as maximum strength predictions. However, simplifying assumptions of various degree can be made, which may reduce the amount of necessary numerical operations to such a level that these methods may be used without the computer for practical estimates or for design. Thus, for small and medium-size rolled H-shapes it may be shown [13] that the following equation approximates the tangent modulus load

$$\frac{P_{TM}}{A} = \frac{\pi^2 E \left( \frac{E_t}{E} \right)}{(L/r)^2} \quad \text{for major-axis bending}$$

and

$$\frac{P_{TM}}{A} = \frac{\pi^2 E \left( \frac{E_t}{E} \right)^3}{(L/r)^2} \quad \text{for minor-axis bending.}$$

where  $E_t$  is the tangent modulus of the complete cross section. Figure 6 gives the computational procedure schematically.

For maximum strength predictions, the approximate method discussed in Refs. 8 and 10 may be sufficiently accurate and useful for many practical purposes. The method is based upon the assumption that the initial deflected curve and the curvature under load may be described by half-sine waves. The mid-height section of the column is considered only. By differentiating the deflected curve function twice, it is possible to obtain a simple relationship between the deflection at mid-height of the column ( $\delta_{mh}$ ) and the curvature at the same point ( $\phi_{mh}$ )

$$\phi_{mh} = \frac{\pi^2}{L^2} \delta_{mh}$$

After choosing arbitrarily a value of  $\delta_{mh}$ , the corresponding curvature  $\phi_{mh}$  is obtained directly from the equation above. The axial strain which produces equilibrium in the cross section can be found by an iterative procedure. The iteration is continued until an equilibrium equation for the mid-height section of the column, that is,

$$P (\delta_{init} + \delta_{mh}) = M$$

is satisfied.  $P$  is the axial load,  $\delta_{init}$  the initial mid-height deflection and  $M$  the internal moment corresponding to the stress distribution in the mid-height section.

Since methods are now available for a more rational column design procedure, there is no longer any need for complicated formulas using various correction factors for estimated fictitious eccentricities or initial deflections--in the past, such factors had been determined to take into account the transition in the column curve from the Euler curve to the yield strength load for short columns. It seems more logical to base an accurate column analysis upon the actual conditions, including measured or estimated residual stresses, out-of-straightness, and mechanical properties.

#### SOME TEST RESULTS: COMPARISONS WITH THEORY

Figures 7 through 12 illustrate the effect of various parameters on the column strength. The diagrams are included here to illustrate a few important points related to the effect of variations in residual stresses due to different manufacturing and fabrication conditions of steel columns.

A comparison between column test results for rolled wide-flange shapes and welded shapes of H and box section, built up from universal-mill plates, is shown in Fig. 7. [14] It is apparent from the diagram that there is a substantial variation between the results obtained for these four kinds of columns. The data of the rolled shapes, all of small to medium-sized cross section, fall reasonably close to the CRC Basic Column curve, suggested by the Column Research Council to describe the strength of columns, [15] and adopted as the design curve by the American Institute of Steel Construction. On the other hand, all the data points for welded shapes are below this curve, for some cases by as much as 30 per cent.

The effect of the column bending axis on column strength is shown in Fig. 8 for rolled wide-flange shapes. [16] Normally, such shapes will have compressive residual stresses at the flange tips, [5,12,13,16] which will reduce the column strength comparatively more for buckling about the minor axis.

Figure 9 shows the effect of the geometrical size of the cross section. Theoretical studies had indicated that the size of a hot-rolled member is an important variable in the formation of residual stresses--the stresses tend to increase with increasing size of a rolled member. [12] This would lead to reduced column strength for heavy rolled columns. The curves in Fig. 9 are tangent modulus predictions based upon the residual stresses predicted in a heavy rolled "jumbo" section 14WF730 and a smaller rolled H-shape. [11,17] It should be noted that the situation probably will be the opposite for welded shapes, because of the fact that welding residual stresses will decrease with increasing size of the structural member. [2]

An important factor which will affect the strength of welded H-columns is the manufacture of the component plates prior to welding. Several tests have shown that flame-cut plates show a more favorable residual stress distribution, which leads to improved strength of H-columns fabricated from such plates, as compared to similar columns built up from universal-mill plates. [10] See Fig. 10. The diagram in Fig. 10 also shows that the tangent modulus prediction estimates the column strength of the flame-cut welded shapes

fairly well. This means that the post-buckling reserve above the tangent modulus load of a fictitious perfectly straight column is of approximately the same magnitude as the reduction in strength due to unintentional out-of-straightness of a practical column. Thus, the tangent modulus concept may be used for the design of such members, including the effect of residual stresses. For the shapes of universal-mill plates in Fig. 10, the post-buckling reserve is considerable and an accurate maximum strength analysis is necessary to obtain close correlation with data.

Figure 11 illustrates the effect of the yield strength level on column strength. [18] Generally speaking, the higher the yield strength, the greater is the column strength, also when compared on a non-dimensional basis as in Fig. 11. The effect may be attributed to the fact that the magnitude of residual stresses often is relatively independent of the yield strength of the steel. [18] Thus, the residual stress to yield strength ratio will be lower for high-strength steels, leading to improved column strength. This trend is accentuated further for quenched and tempered steels, such as A514 steel, which have comparatively small magnitudes of residual stress due to the heat treatment.

Figure 12 shows the column strength of shapes which have been specially treated after manufacture--by an annealing that removes the major portion of residual stresses, and by a reinforcement accomplished merely by laying a weld bead along the flange tips. [19] The improved strength in the reinforced columns is achieved through the reversal of residual stresses at the flange edges.

### CONCLUSIONS

Methods for forecasting the structural behavior of steel columns based upon variations in different relevant parameters, in particular residual stresses, have been discussed in this paper. Examples were given for the influence of various parameters on column strength. The results indicate that the strength and behavior of columns under load can be predicted, and that the various influencing factors may be included in the prediction. While a summary of all column tests shows a tremendous scatter, most of this variation can be attributed to parameters which may be controlled in the design and fabrication. Thus, methods and extensive data are available for the rational design of centrally loaded steel columns.

The large scatter in results, and the consideration that this variation is caused largely by controllable factors, makes clear that the use of one design curve for all columns penalizes certain groups of columns, whereas other types of columns having a comparatively low strength will be designed to a lower real factor of safety. It appears logical that the specifications for the design of columns should be reconsidered in this light.

### ACKNOWLEDGEMENTS

This paper presents the results of a long-term study into the column strength of structural steel members, underway at Fritz Engineering Laboratory, Lehigh University, Bethlehem, Pennsylvania. The National Science

Foundation sponsored the most recent part of the study.

Acknowledgements are due to the many colleagues who contributed to the various phases of the study and to whose work reference was made in the paper. In particular, Lynn S. Beedle, Director of Fritz Engineering Laboratory, provided guidance in the early stages of the investigation, and inspiration throughout the course of the study.

#### REFERENCES

1. L. Tall and G. A. Alpsten  
ON THE SCATTER IN YIELD STRENGTH AND RESIDUAL STRESSES IN STEEL MEMBERS, Fritz Engrg. Lab. Report No. 337.22, Lehigh University; to be presented at the IABSE Symposium, Theme IVa, London, September 1969.
2. G. A. Alpsten and L. Tall  
RESIDUAL STRESSES IN HEAVY WELDED SHAPES, Fritz Engrg. Lab. Report No. 337.12, Lehigh University, January 1969; to be published in the Welding Journal.
3. F. R. Estuar and L. Tall  
TESTING OF PINNED-END STEEL COLUMNS, Test Methods for Compression Members, ASTM STP 419, American Society for Testing and Materials, 1967.
4. W. R. Osgood  
THE EFFECT OF RESIDUAL STRESS ON COLUMN STRENGTH, Proc., First National Congress Applied Mechanics, June 1951.
5. C. H. Yang, L. S. Beedle and B. G. Johnston  
RESIDUAL STRESS AND THE YIELD STRENGTH OF STEEL BEAMS, The Welding Journal, Vol. 31 (4), 1952.
6. A. W. Huber and R. L. Ketter  
THE INFLUENCE OF RESIDUAL STRESS ON THE CARRYING CAPACITY OF ECCENTRICALLY LOADED COLUMNS, IABSE Publications, Zurich, December, 1958.
7. Y. Fujita  
ULTIMATE STRENGTH OF COLUMNS WITH RESIDUAL STRESSES, Journal, Society of Naval Architects of Japan, January 1960.
8. L. Tall  
THE STRENGTH OF WELDED BUILT-UP COLUMNS, Ph.D. Dissertation, Lehigh University, May 1961; University Microfilms, Inc., Ann Arbor.
9. R. H. Batterman and B. G. Johnston  
BEHAVIOR AND MAXIMUM STRENGTH OF METAL COLUMNS, Journal of the Structural Division, Proc. ASCE, Vol. 93, ST2, April 1967.
10. R. K. McFalls and L. Tall  
A STUDY OF WELDED COLUMNS MANUFACTURED FROM FLAME-CUT PLATES, The Welding Journal, Vol. 48 (4), April 1969.

11. G. A. Alpsten and L. Tall  
COLUMN STRENGTH OF HEAVY SHAPES - A PROGRESS REPORT, Fritz  
Engrg. Lab. Report No. 337.16, In preparation.
12. G. A. Alpsten  
THERMAL RESIDUAL STRESSES IN HOT-ROLLED STEEL MEMBERS, Fritz  
Engrg. Lab. Report No. 337.3, December 1968; to be published  
in the Welding Journal.
13. A. W. Huber and L. S. Beedle  
RESIDUAL STRESSES AND THE COMPRESSIVE STRENGTH OF STEEL, The  
Welding Journal, Vol. 33, December 1954.
14. F. R. Estuar and L. Tall  
EXPERIMENTAL INVESTIGATION OF WELDED BUILT-UP COLUMNS, The  
Welding Journal, Vol. 42, April 1963.
15. B. G. Johnston (Ed.)  
GUIDE TO DESIGN CRITERIA FOR METAL COMPRESSION MEMBERS, Column  
Research Council, 2nd Ed., Wiley, 1966.
16. L. S. Beedle and L. Tall  
BASIC COLUMN STRENGTH, Journal of the Structural Division,  
Proc. ASCE, Proc. Paper 2555, Vol. 86 (ST-7), July 1960.
17. G. A. Alpsten  
EGENSPÄNNINGAR I VARMVALSADE STÄLPROFILER ("RESIDUAL STRESSES  
IN HOT-ROLLED STEEL PROFILES"), Institution of Structural  
Engineering and Bridge Building, Royal Institute of Technology,  
Stockholm, June 1967.
18. Y. Kishima, G. A. Alpsten and L. Tall  
RESIDUAL STRESSES IN WELDED SHAPES USING FLAME-CUT PLATES,  
Fritz Engrg. Lab. Report No. 321.3, Lehigh University, In  
preparation.
19. L. Tall  
WELDED BUILT-UP COLUMNS, Fritz Engrg. Lab. Report No. 249.29,  
Lehigh University, April 1966.

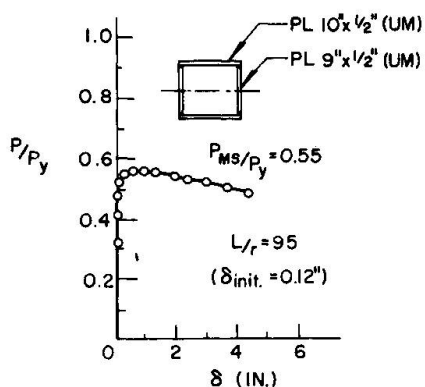


Fig. 1 Schematic load-deflection curves for simple columns

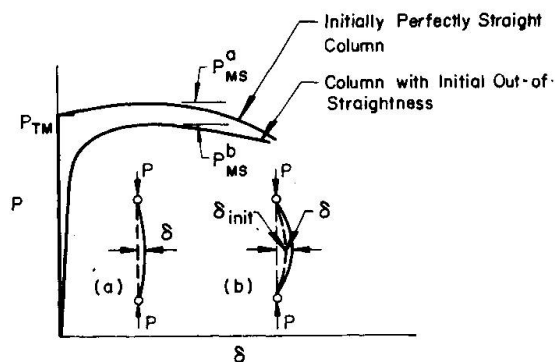


Fig. 2 Experimental load-deflection curve for a centrally loaded column

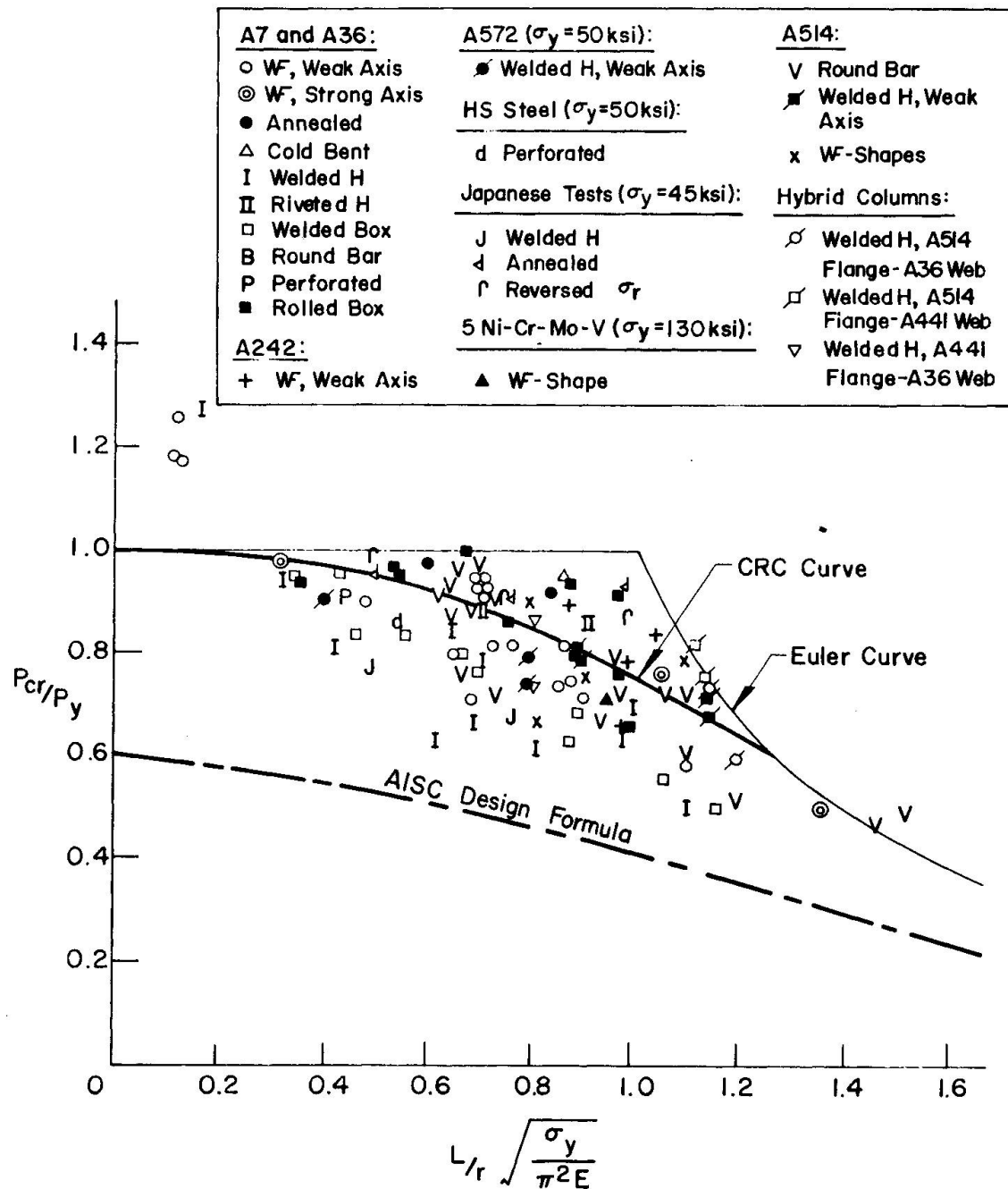


Fig. 3 Column test results



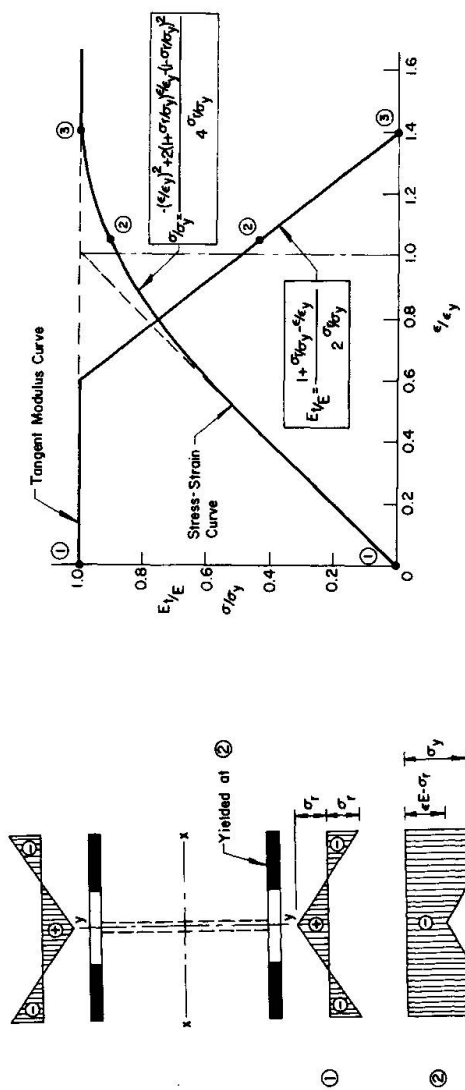


Fig. 4 Typical tangent modulus curves for a rolled WF-shape

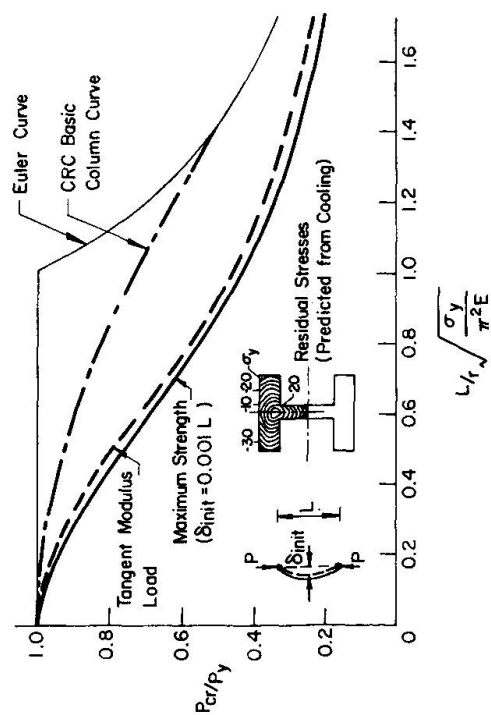


Fig. 5 Maximum strength curve for a heavy rolled "jumbo" shape 14WF730, weak axis

(a) Total Stress Distribution

(b) Stress-Strain and Tangent Modulus Curves for Cross Section

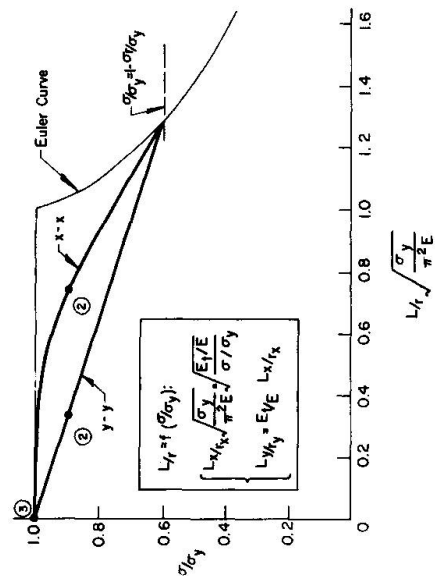


Fig. 6

Principle of approximate method for tangent modulus analysis

(c) Column Curves

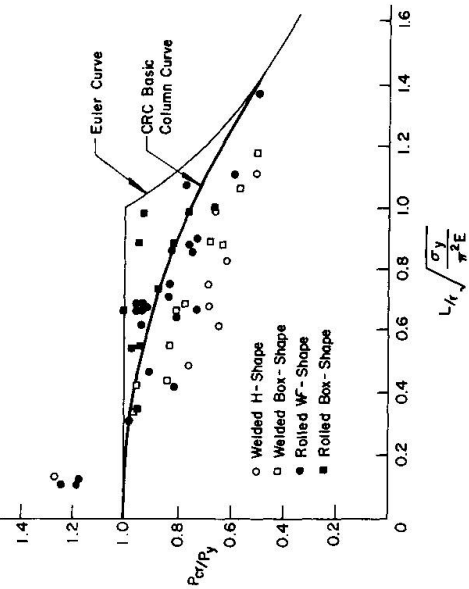


Fig. 7 Column test results for rolled and welded shapes

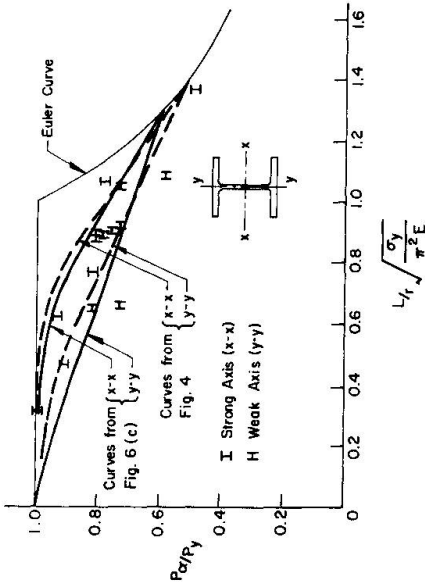


Fig. 8 Effect of bending axis on column strength, rolled WF-shapes

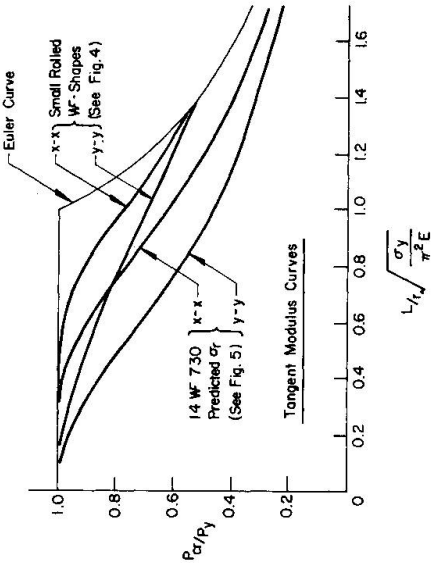


Fig. 9 Effect of geometrical scale of cross section on column strength

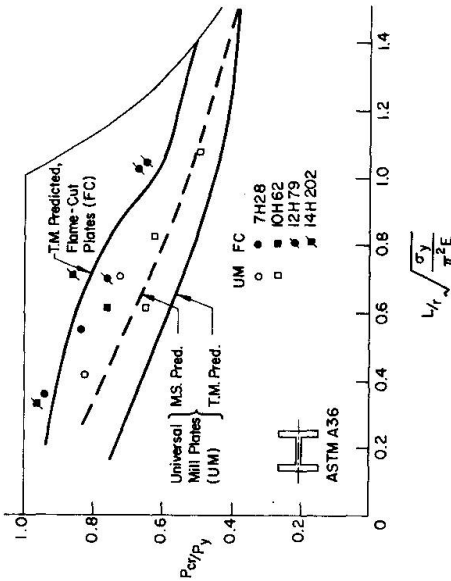


Fig. 10 Column strength of welded H-shapes of flame-cut and universal-mill plates.

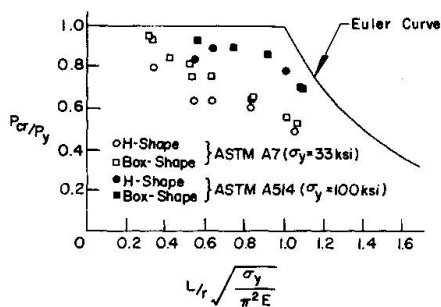


Fig. 11 Effect of yield strength on column strength

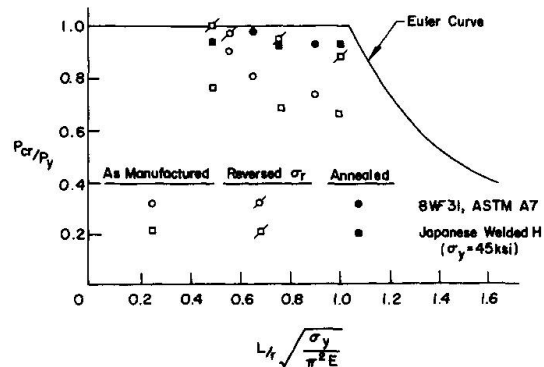


Fig. 12 Strength of H-columns; as manufactured, with reversed residual stress, and annealed

## SUMMARY

The discussion summarizes some results obtained in a study of residual stresses and column strength of rolled and welded steel shapes. Methods for forecasting the structural behavior and maximum strength of steel columns based upon variations in different relevant parameters, in particular residual stresses, are reviewed. Examples are given for the influence on column strength of various parameters, including manufacturing and fabrication procedures, bending axis, geometry of cross section, yield strength, and strengthening operations.

## RESUME

Les résultats obtenus lors d'une étude sur les contraintes résiduelles et la résistance des poteaux laminés ou reconstitués sont discutés. Quelques méthodes pour déterminer le comportement de la charge ultime des poteaux en acier, selon différents paramètres pertinents, en particulier celui des contraintes résiduelles sont revues. Plusieurs exemples montrent l'influence des paramètres sur la résistance des poteaux. Les paramètres étudiés sont les procédés de fabrication, l'axe d'inertie, la géométrie de la section droite, la limite d'élasticité et les opérations de redressement.

## ZUSAMMENFASSUNG

Dieser Beitrag fasst jene Ergebnisse zusammen, die durch Untersuchungen über die Eigenspannungen und über das Tragverhalten an gewalzten und geschweissten Stahlprofilen erhalten wurden. Es werden Berechnungsmethoden für die Voraussage des Tragverhaltens und der Traglast aufgrund der Veränderung wichtiger Parameter, insbesondere der Eigenspannungen, behandelt. Beispiele zeigen den Einfluss der verschiedenen Parameter—einschliesslich Bearbeitungs- und Herstellprozess, Knickachse, Geometrie des Querschnittes, Streckgrenze und Reckungen— auf die Stützspannung.

## **Flexural and Torsional Failure Modes of Continuous Thin Walled Beams**

Les différents cas de ruine des poutres continues à parois minces soumises à la flexion et à la torsion

Biege- und Drillbrucharten durchlaufender dünnwandiger Stäbe

**M.M. BLACK, D.A. NEWTON and H.M. SEMPLE**

Structural Mechanics Research Group  
University of Sussex, England

### Introduction

The work described in this contribution has been undertaken as a follow up to an investigation into the stress systems obtaining in continuous thin walled structural systems subjected to combined bending and torsion. Although the project is in its early stages it was felt that the results already noted gave some indication of the complexity of the problem and if published, might encourage further research in other centres.

It is well known that cold formed thin walled sections are, by reason of their cross-sectional form, subjected to both bending and torsion in any practical application. This kind of loading produces localised high stress values which if used for an elastic design procedure can give rise to rather conservative section sizes. One approach to overcoming this difficulty is by bracing the member in such a way as to reduce the longitudinal torsional stresses. (1) Such techniques will of course lead to higher construction costs. It is possible that given a better understanding of the localised high stresses and the resulting flange buckling, a design procedure analogous to the collapse approach used in plastic design of conventional hot rolled sections, could be developed. In this way more economic use could be made of thin walled sections and their field of application increased.

It is immediately obvious that the concept of the 'plastic hinge' used in the collapse method of analysis cannot apply directly to thin walled sections. However, as will be seen from the tests described later, the overall mechanism of collapse of a thin walled continuous beam is of the same form as that occurring when a conventional hot rolled section is used. In the case of a thin walled element the plastic hinge would appear to be replaced by gross cross-sectional deformation arising from local flange buckling combined with the initiation of some plastic flow in the material.

At the present time the emphasis of the research programme is on the experimental work and this is reflected by the contents of this contribution. Theoretical analysis is of course being developed and a brief indication of this part of the programme is also included in the closing summary.

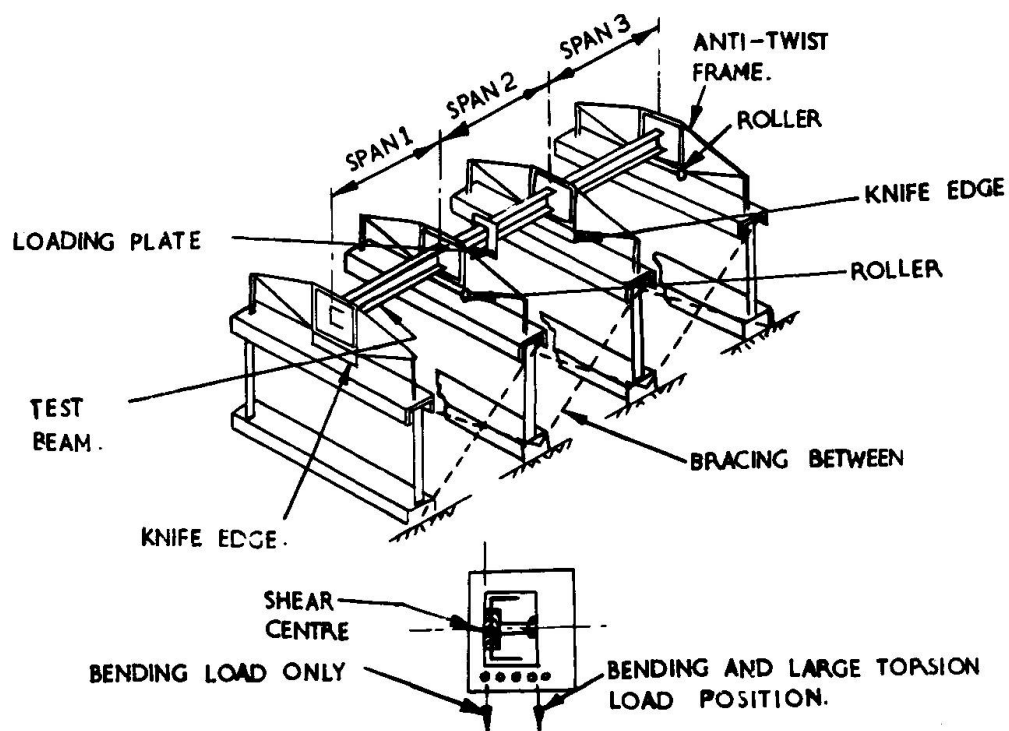
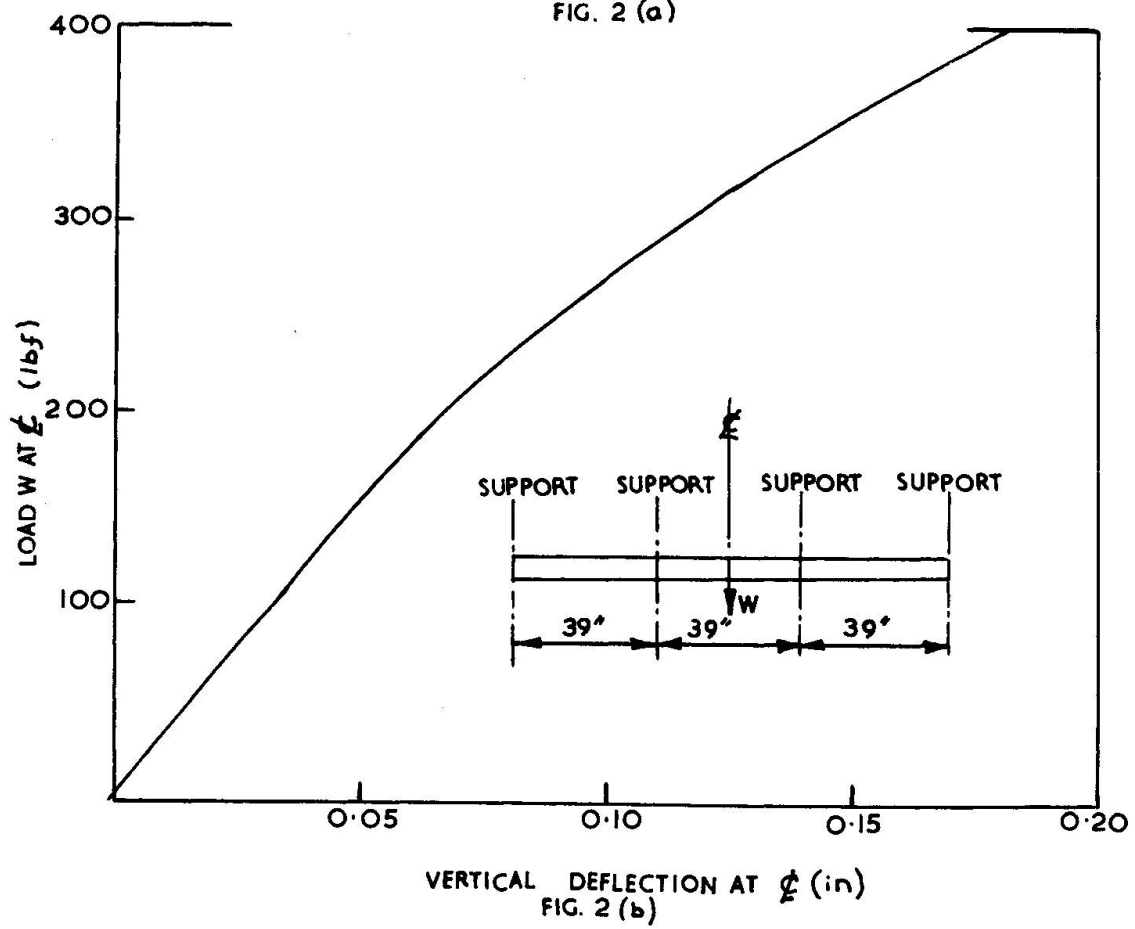
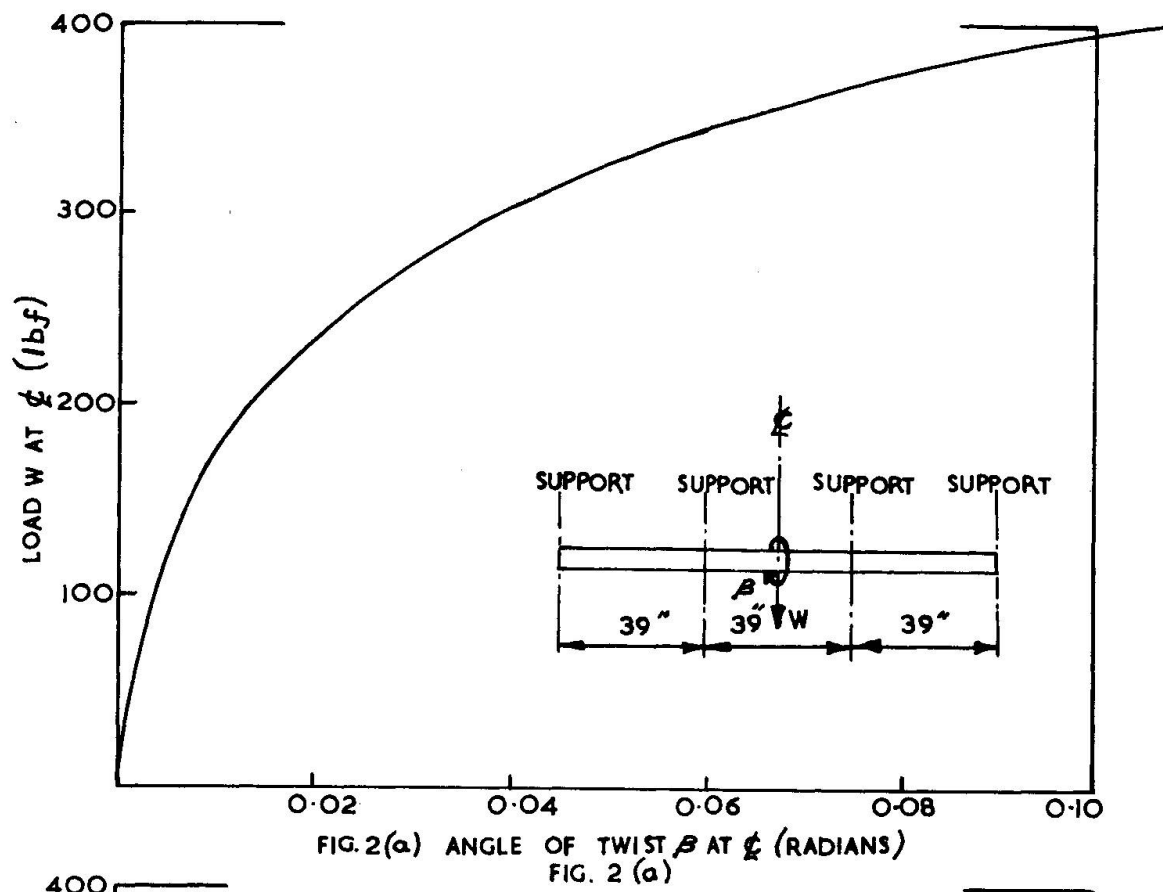


FIG. 1. DETAILS OF CONTINUOUS BEAM TEST RIG.





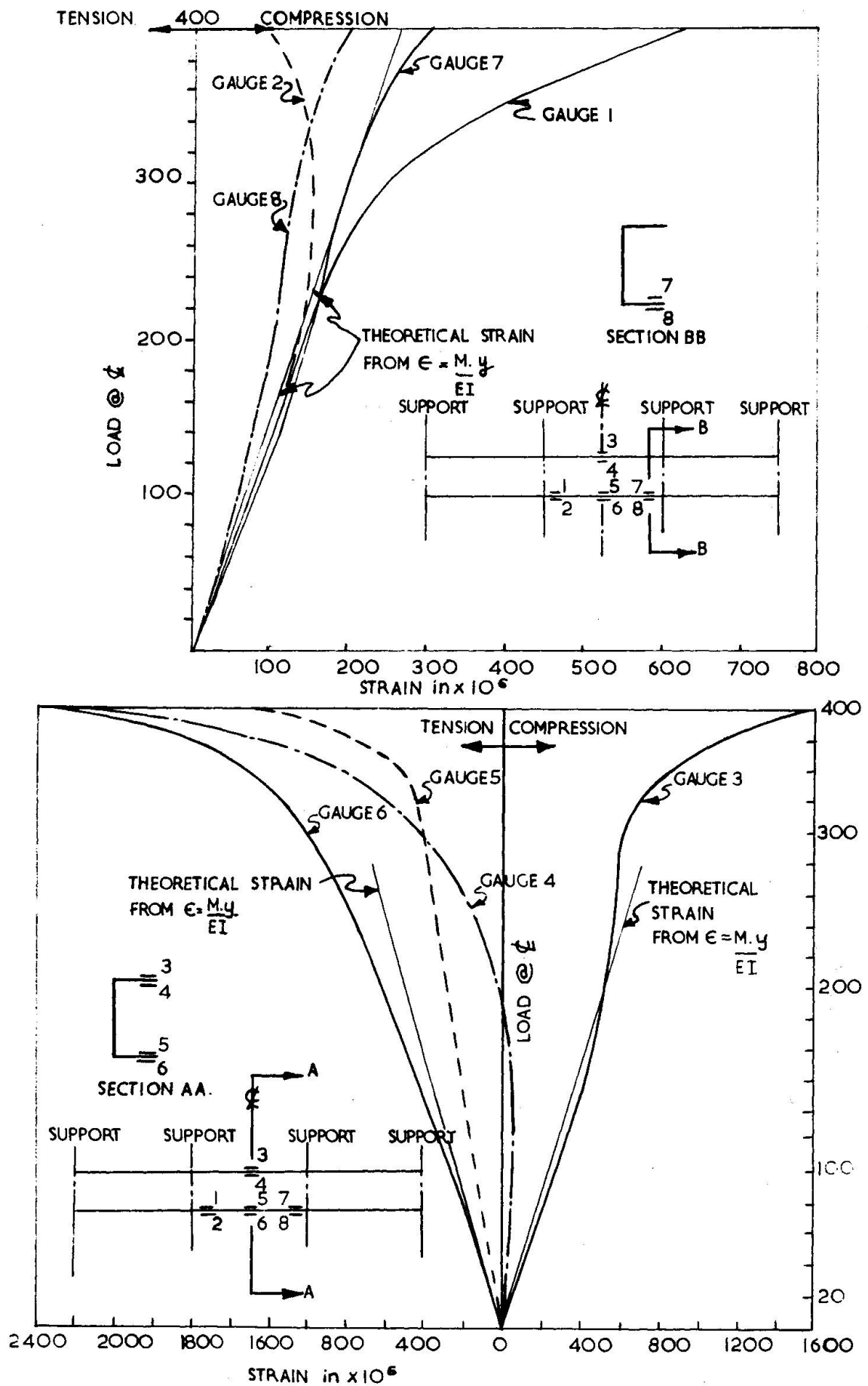


FIG. 3.

### Experimental Programme

A series of tests to failure were carried out on 120 inch lengths of 2 inch by 1 inch cold formed mild steel channel sections. Two thicknesses of material were used; 0.025 inches and 0.035 inches. The beams were supported in four diaphragms each 39 inches apart. This gave rise to a three span continuous beam configuration as shown in Fig. 1. The diaphragms prevented vertical and horizontal deflection and twist in the plane of the section.

Loads were applied at the centre of the middle span by means of a disc or plate clamped to the web of the beam. Using a disc with its centre arranged to coincide with the shear centre of the section pure torque about this point was applied.

For bending, loads were suspended from a plate clamped to the web of the section with the weight hanger in the vertical plane containing the shear centre. By carrying the lateral position of this weight hanger it was possible to produce the third loading condition, that of combined bending and torsion. Recordings of vertical deflection and angle of twist at the centre of the middle span were taken at each movement of load. In addition strain gauge readings at eight critical flange positions for each load increment, were taken during the 'pure' bending tests. The strain gauges used were of the 'foil yield' type and can measure strains ranging from 10% to 20%.

### Experimental Results

#### i) Pure Bending

As already noted the loading for this form of test was in the plane of the shear centre. It is however appreciated that the reaction forces at the diaphragm supports would not be in this same plane. This would lead to some small increments of torque and resulting twist being present during the tests. In fact as can be seen from Fig. 2 (a) the angle of twist at the centre of the middle span during one of the 'pure' bending tests was approximately 0.016 radians at 220 lbf and 0.1 at 400 lbf. This particular beam finally collapsed at a load of 435 lbf.

In all the 'pure' bending tests the mechanism of collapse was the same. Thus a collapse 'hinge' formed first at the centre of the middle span and then complete failure occurred when two such 'hinges' formed close to the two internal supports. A beam after failure is shown in Fig. 4.(b)

This form of collapse mechanism is similar to that assumed for this case in standard limit analysis theory. The collapse hinges, however, appeared to be the result of gross geometric deformations of the cross-section which result in a reduction of the bending stiffness together with the development of plasticity in the material.

The effect of local bending in the flanges which finally produces local flange buckling is clearly seen from the strain gauge results shown in Fig. 3. At the centre of the middle span local bending of the compression flange commences at the first load increment and increases rapidly with load. In the results shown the underside of the top flange (Gauge 4) had actually gone into tension at half the collapse load (approximately 220 lbf) On offloading from this position the beam returned to its initial state indicating the elastic nature of this local deformation at this stage.

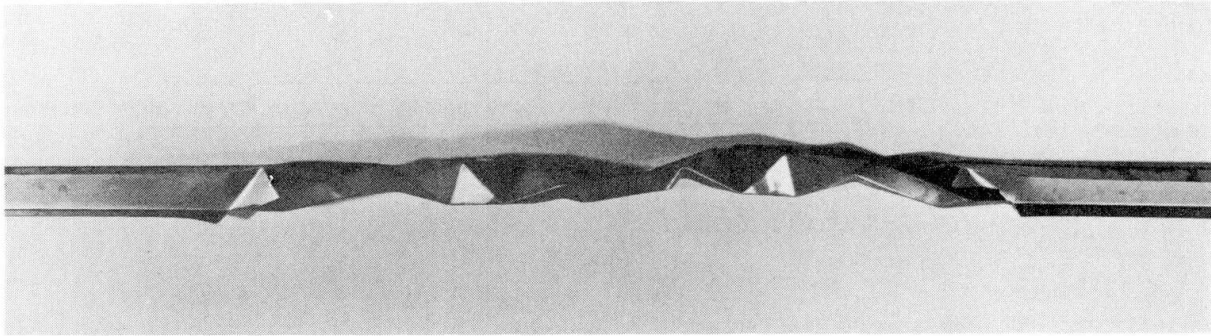


FIG. 4 (a) PURE TORSION COLLAPSE.

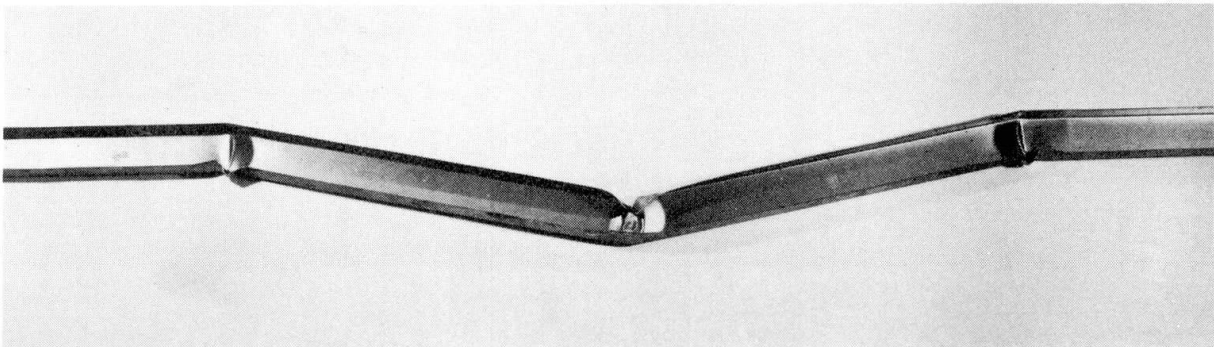


FIG. 4 (b) PURE BENDING COLLAPSE.

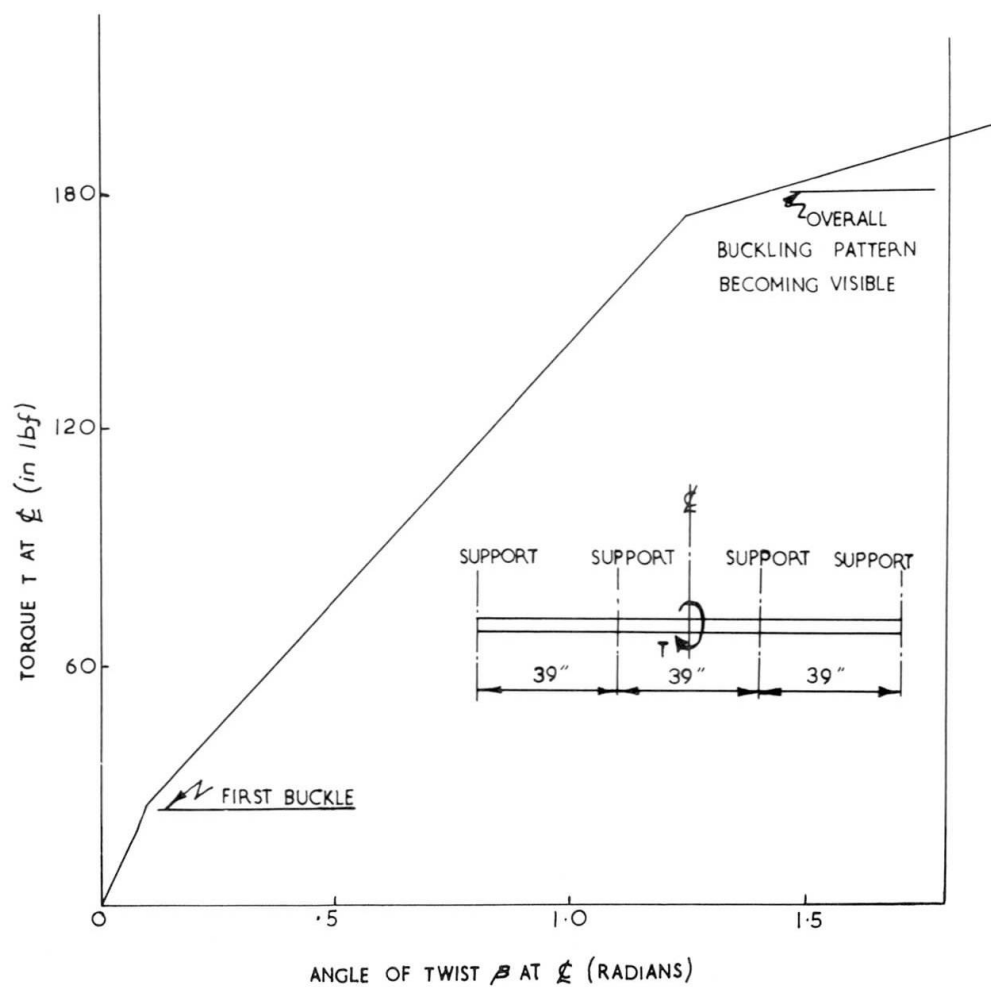


FIG. 5.

As would be expected the effect is much less pronounced in the tension flange (Gauges 6 and 6) and also in the compression flange near the internal supports (Gauges 1, 2, 7 and 8).

The vertical deflection at the local position (Fig. 2 (b)) increased almost linearly until collapse occurred at which stage it increased too rapidly to be recorded. However at a load of 400 lbf, only 35 lbf less than the collapse load, the deflection was as little as 0.18 inches, that is approximately  $1/220$  of the span.

#### ii) Pure Torsion

In this series of tests the effect of local buckling was also very pronounced. A typical torque/angle of twist equilibrium path at the centre of the middle span is shown in Fig. 5. Initially a local buckle formed adjacent to the loading disc of a relatively low value of applied torque (24 in lbf). Further increases in torque gave rise to a linear torque/angle of twist relationship until the initial stages of the failure mechanism became apparent (180 in lbf). Thereafter the angle of twist increased rapidly until failure occurred (204 in lbf). At failure the deformations took the form of a very distinct pattern of web buckling. The lines formed by the buckles divided the web of the middle span into a uniform series of triangular areas as shown in Fig. 4(a).

The failure mode was again considered to be a combination of gross geometric deformation of the cross-section and the development of zones of plastic material.

#### iii) Combined Bending and Torsion

As would be expected the collapsed form of the beams when subjected to combined bending and torsion indicated the same gross geometric cross-sectional deformations and development of plasticity in the material. Theoretically, longitudinal warping stresses due to torsion initiate local flange yielding at lower values of load than in the corresponding 'pure' bending case. However the final collapse loads were not significantly different when the load to produce the combined effects was acting in the vertical plane containing the centroid of the section. This form of loading is perhaps closest to that obtaining in any practical situation using such sections.

#### Summary and Conclusions

The test results have indicated clearly that final collapse for all three forms of load action resulted from a combination of elastic instability, in-plane cross-sectional deformation and some plastic flow. It was obvious that the standard 'plastic hinge' concept was not directly applicable in this case.

As would be expected local flange bending and buckling play a prominent part in the collapse at any section. At critical positions of maximum bending moment and torsional bi-moment, local bending effects are initiated at very small loads. They are not visible at this stage but are easily observed from the strain gauge readings. Such effects become visible at higher loads in the form of a pronounced local buckle. At this stage the magnitude of the local flange deflection is many times greater than the material thickness.

Some typical results from the tests are given in the following table. The first group correspond to 'pure bending' loads and the second to combined bending and small torsion, that is, the loads acting in the vertical plane containing the centroid. The two figures in the last column are the values of load for each group required to develop the yield stress at the centre of the middle span. The values are calculated from linear-elastic analysis and the lower load for the combined actions arises from taking into account the longitudinal warping stresses due to torsion.

Group	First Buckle Load	Collapse Load	Theoretical First Yield Load
1	110	200	226
	131	197	
	141	219	
2	191	226	91
	121	192	
	131	197	

TABLE 1 (All loads given in lbf)

From this table it can be seen that (i) as already noted there is no significant difference in collapse loads for the two different forms of loading and (ii) although theoretically the warping stresses produce local yielding at lower loads this does not significantly affect the load required for developing the first buckle.

In relation to this latter comment it must be noted that longitudinal warping stress distribution round the cross-section gives a maximum value at the free edge of the flange and reduces rapidly towards the web to flange junction at which point it will have changed sign. A detailed analysis of such stress in thin walled continuous beams subjected to bending and torsion has been presented elsewhere (2,3). However as these effects are highly localised they will tend to give rise to conservative safe loads if used in standard elastic design procedures.

It is possible that by adopting a design procedure based on collapse more economic use can be made of thin walled sections. The obvious difficulty is the prediction of the collapse loads for such sections. The stress distributions for combined bending and torsion are highly non-uniform which makes the evaluation of critical compressive stresses in the flanges very complex. In addition gross cross-sectional deformations which occur locally in flanges prior to collapse are, as already noted, many times greater, than the material thickness. This implies that the flange, considered as a plate element, is in the non-linear behavioural range. Thus, the value of collapse loads are unlikely to be predicted by any method which is based on a linear theory. Local imperfections will also influence the behaviour particularly in the non-linear range.

However the results of tests so far have shown reasonable repeatability of both collapse forms and ultimate loads. They have also indicated a considerable post local buckling load carrying capacity. It does not seem unreasonable therefore that design criteria, which allow for elastic instability, post critical load carrying capacity and some measure of plastic flow, can be developed.

### Bibliography

1. V.Z. VLASOV 'Thin-walled elastic beams', programme for scientific translations, Jerusalem, Israel, 1961.
2. M.M. BLACK and H.M. SEMPLE 'Thin-walled elements in the design of structural systems', Iron and Steel Institute, Publication 119, Proceedings of Symposium, 'Challenge for Steel'.
3. M.M. BLACK and H.M. SEMPLE 'Torsion-bending analysis of continuous thin-walled beams'. Int. Jnl. Mech. Sci, 1969 (to be published).

## SUMMARY

This contribution concerns an investigation into the mechanism of collapse of thin walled continuous beams. Three forms of load action are considered; pure bending, pure torsion and combined bending and torsion. All tests were continued until collapse occurred, this condition being defined as the state at which no further load could be carried. Details are given of deflections, angles of twist and strain gauge readings, observed during the tests. The experimental results illustrate the complexity of the failure modes. As a result some indication is given of the factors to be considered in the development of adequate design criteria.

## RESUME

Le présent article étudie les modes de ruine des poutres continues à parois minces. On considère trois sortes de sollicitations: flexion simple, torsion et combinaison des deux cas. Tous les essais ont été effectués jusqu'à l'état de ruine, défini par le point où la poutre ne supportait plus une augmentation de charge. On indique en détail les flèches, les angles de torsion et les lectures sur les "strain gauges" durant les essais. Les résultats expérimentaux illustrent la complexité des cas de ruine. En conclusion, on étudie les facteurs importants pour le développement des critères de construction.

## ZUSAMMENFASSUNG

Dieser Beitrag schildert die Untersuchungen über die Mechanismen der plastischen Gelenke bei dünnwandigen, durchlaufenden Balken. Drei Lastfälle sind betrachtet worden: Reine Biegung, reine Drillung und die Kombination derselben. Alle Prüfungen sind bis zum Kollaps (Zusammenbruch) durchgeführt worden, der für jenen Zustand definiert wurde, da keine weitere Last mehr angebracht werden kann. Durchbiegungen, Drehwinkel und Dehnungsmesstände während des Prüfverlaufs werden angegeben. Die experimentellen Ergebnisse verdeutlichen die vielfältigen Zusammenhänge der Brucharten. Als Ergebnis werden einige Punkte aufgezeigt, die beim angemessenen Entwurf berücksichtigt werden sollten.



Leere Seite  
Blank page  
Page vide

## Computer Experiments Concerning Random Nonlinear Structural Behaviour

Expériences sur ordinateur concernant le comportement aléatoire non-linéaire des structures

Rechnerexperimente für zufälliges, nichtlineares Bauwerkverhalten

**JÚLIO FERRY BORGES**

Associate Director  
Laboratório Nacional de Engenharia Civil  
Lisbon, Portugal

**DONALD J. BUTLER**

Professor of Civil Engineering  
Rutgers University  
New Brunswick, New Jersey, U.S.A.

### 1 – INTRODUCTION

While rational probabilistic approaches to questions of structural safety and reliability have received considerable attention in recent years, the actual application of such concepts in practical structural design has been quite limited. Certainly part of the reluctance to employ probabilistic concepts in practice is explained by the inadequate state of our knowledge concerning the statistical character of structural loading and structural behaviour. While the stochastic character of the loads acting on structures must presumably be deduced from field observations, it is not likely that statistically meaningful information on structural behaviour, for structures of any complexity, can be obtained from field or laboratory tests because of practical limitations on the size of the statistical samples available.

These considerations suggest that it would be of value to develop analytical methods which would enable one to predict stochastic structural response characteristics from the knowledge of variability in the properties of structural materials. At present such a statistical theory of structures exists only for the study of brittle behaviour. It was established by Weibull (1). For other types of material behaviour, some particular results have been obtained (2).

The present paper employs a previously suggested numerical approach (3) to study randomness in the nonlinear behaviour of plane skeletal structures. A computer program developed to analyse framed structures possessing rather arbitrary nonlinear moment-curvature relations (4) is utilised to study the flexural behaviour of samples of randomly formed, nominally identical structures. The randomness considered derives from the uncertain nature of the mechanical properties of the materials, as reflected in the moment-curvature diagrams of the unit elements used to form the structures; structure geometry as well as conditions of loading and support are

considered to be deterministic. The intent is thus to examine the manner in which the stochastic character of structural behaviour is influenced by the probabilistic nature of material properties.

In the examples presented, the element moment-curvature diagrams were assumed to belong to a prescribed statistical populations and prismatic beams were formed by combining elements chosen at random from this population. The tri-linear diagrams employed closely represent the nonlinear behaviour to be expected in conventionally reinforced concrete beams (5). The distribution of  $M$  for a given curvature was assumed to be Gaussian with a coefficient of variation of 10%. Load-deflection curves were determined for a sample of twenty beams, each containing forty elements, under several conditions of loading and support.

While the examples considered are relatively simple, it is felt that they offer some insight into the little understood subject of random nonlinear behaviour. The proposed method of computer simulated numerical experiments may be readily extended to include more general structures and statistical distributions.

## 2 - RANDOMNESS OF MOMENT-CURVATURE RELATIONS AND OF STRUCTURAL BEHAVIOUR

If several nominally identical flexural elements are tested in pure bending in the same manner, different moment-curvature relations  $M(\theta)$  will be obtained, Fig. 1a, and a probabilistic distribution may then be defined for the set of relations. In what follows, it is assumed as a working hypothesis that the distribution of  $M$  for a given value of  $\theta$  is normal, with a mean value  $\bar{M}$  and a coefficient of variation  $c_v$  which is independent of  $\theta$ . Thus a particular diagram  $M_i(\theta_i)$  is related to the mean diagram  $\bar{M}(\theta)$  by  $M_i = \bar{M}(\theta_i) (1 + \alpha c_v)$ , where  $\alpha$  measures (in standard deviations) the distance of the considered diagram from the mean diagram. Since the diagrams, in the regions of practical interest, are monotonic, it follows that

$$P_r(M < M_i | \theta_i) = P_r(\theta > \theta_i | M_i)$$

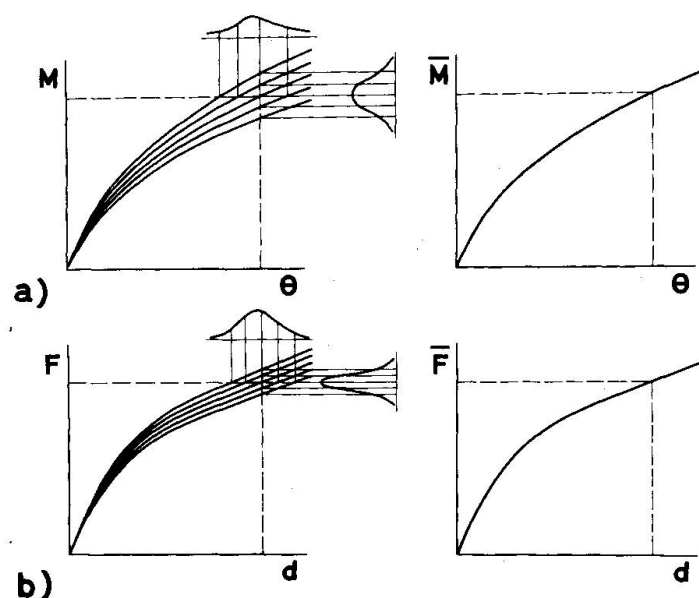


Fig. 1 - Randomness of mechanical properties and of structural behaviour

It should be noted that the distribution of  $\theta$  for a given value of  $M$  is not normal, since this occurs only if the diagrams are straight and parallel.

It is also clear from Fig. 1 that the distribution of  $\theta$  is not symmetrical but is skewed toward the larger values

of  $\theta$ . The dispersion and skewness increase with increasing  $M$ .

Mechanical and statistical considerations suggest that the hypothesis of normality for the distribution  $P_r(M < M_i | \theta_i)$  is a reasonable one. Since the bending moment  $M$  is merely the integral, taken over the cross section, of the stresses developed at elementary areas multiplied by corresponding distances to the neutral line, for a given state of deformation (curvature) the central limit theorem implies an approximately normal probabilistic distribution of  $M$  for the population of unit elements.

If random combinations of these unit elements are used to form a sample of nominally identical structures, the behaviour of these structures under deterministic proportional loading may be investigated numerically and the results obtained represented by a family of force-displacement diagrams, as shown in Fig. 1b. Statistical methods may then be used to study the relation between ran-

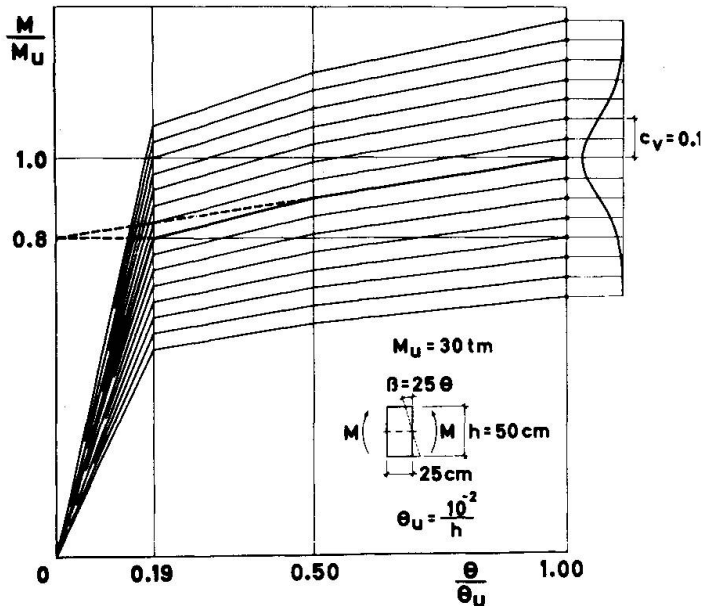


Fig. 2 — Trilinear moment-curvature diagrams.

domness of mechanical properties and randomness of structural behaviour and to investigate questions of structural safety.

The particular  $M(\theta)$  diagrams employed in the examples were of the tri-linear type shown in Fig. 2. The graph shown in heavy outline represents the mean behaviour  $\bar{M}(\theta)$ , while the other diagrams represent a normal population. The coefficient of variation was assumed to be 10%.

### 3 — FORMATION OF BEAMS BY RANDOM SAMPLING

A sample of twenty beams was constructed for the study. To accommodate the available computer program (4), each of the twenty beams was formed by combining 39 whole-length unit elements with two half-length elements, one at each end. The length of the elements was thus 1/40 of the total beam length.

Fifteen different element types, corresponding to fifteen different  $M(\theta)$  diagrams (or fifteen values of  $M_u$ ), were used to form the beams. The diagrams were spaced at intervals of  $.05 \bar{M}$ ; i.e., at intervals of one half of the standard deviation. Each sample beam consisted of a set of 41 elements chosen at random from this population. The selection of the elements was performed with the aid of tables of Random Normal Deviates (6), and the frequency distribution of element types is given in Table 1.

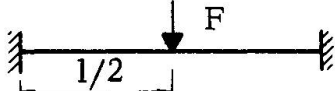
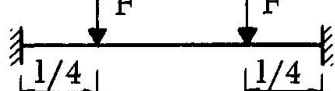
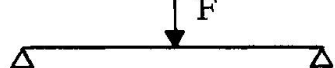
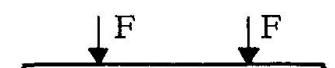
TABLE 1 - ELEMENT TYPES

Element Type	$\frac{M_u}{\bar{M}_u}$	$\alpha$	Corresponding Range of Random Normal Deviate	Normal Frequency of Occurrence %
1	0.65	- 3.5	- $\infty$ to - 3.25	0.06
2	0.70	- 3.0	- 3.25 to - 2.75	0.24
3	0.75	- 2.5	- 2.75 to - 2.25	0.92
4	0.80	- 2.0	- 2.25 to - 1.75	2.79
5	0.85	- 1.5	- 1.75 to - 1.25	6.55
6	0.90	- 1.0	- 1.25 to - 0.75	12.10
7	0.95	- 0.5	- 0.75 to - 0.25	17.47
8	1.00	0	- 0.25 to 0.25	19.74
9	1.05	+ 0.5	0.25 to 0.75	17.47
10	1.10	+ 1.0	0.75 to 1.25	12.10
11	1.15	+ 1.5	1.25 to 1.75	6.55
12	1.20	+ 2.0	1.75 to 2.25	2.79
13	1.25	+ 2.5	2.25 to 2.75	0.92
14	1.30	+ 3.0	2.75 to 3.25	0.24
15	1.35	+ 3.5	3.25 to + $\infty$	0.06

## 4 - TEST STRUCTURES AND NUMERICAL EXPERIMENTS

Numerical experiments on the twenty beams were performed for four different conditions of loading and support as indicated in Table 2 which al-

TABLE 2 - TEST STRUCTURES

Ref. Number	Structure	Span $l$	Depth $h$	Ult. Moment $M_u$
1		10 m	50 cm	$\pm 30 \text{ tm}$
2		10 m	50 cm	$+ 10 \text{ tm}$ $- 30 \text{ tm}$
3		10 m	50 cm	$+ 30 \text{ tm}$
4		10 m	50 cm	$+ 30 \text{ tm}$

so gives the dimensions, mean ultimate moments, and ultimate curvature values used in the computations. Note that the ratio of positive to negative ultimate moments for the hyperstatic structures, 1 and 2, is based

upon elastic design requirements.

Deflections at regular increments of increasing load were determined using two computer programs developed at LNEC for the nonlinear analysis of either isostatic or hyperstatic plane framed structures. Each permits the introduction of numerous arbitrary  $M(\theta)$  data defining the nonlinear flexural behaviour of the various element types that make up the structure. For isostatic cases, deflections are obtained by a simple numerical integration of the beam differential equation,  $y'' = \theta$ , satisfying the appropriate boundary conditions. For hyperstatic cases, an iterative procedure based on the stiffness method is used to determine displacements, moments and shears for each level of loading. This program is described in considerable detail in a previous paper (4).

## 5 — RESULTS OF SIMULATED TESTS

The load-deflection data obtained for the four structures are presented graphically in Figs. 3, 4, 5 and 6. In addition to the twenty graphs for the

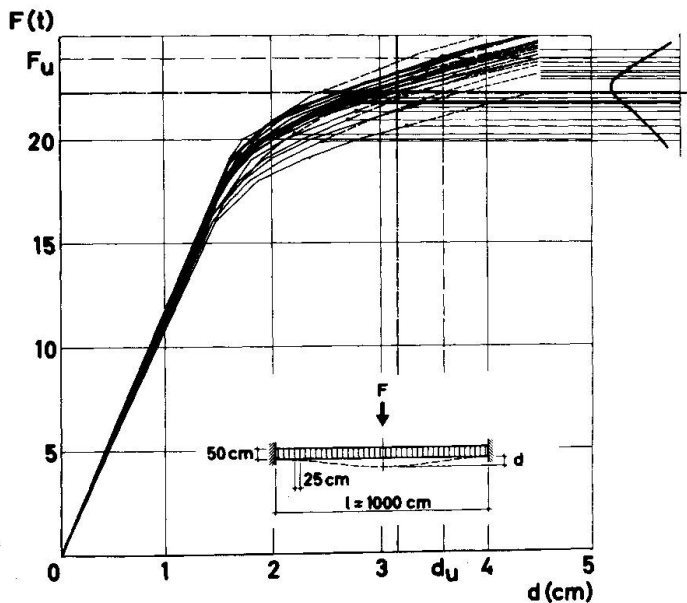


Fig. 3 — Load-deflection diagrams for structures 1.

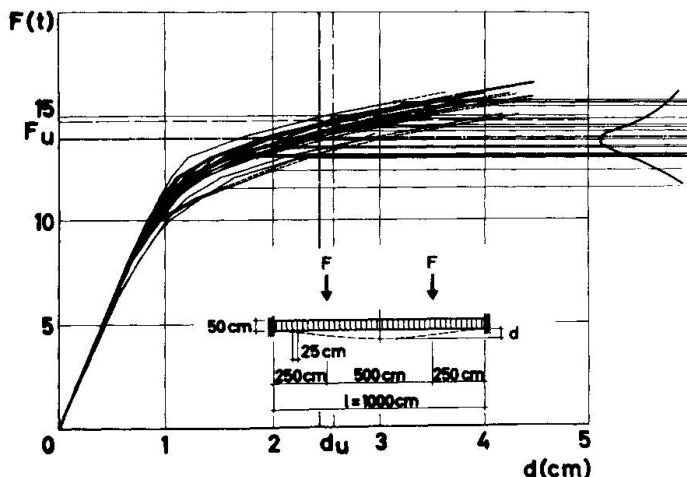


Fig. 4 — Load-deflection diagrams for structures 2.

sample beams, the figures show, in heavier outline, the diagrams obtained for a "standard" beam which possesses uniform mechanical properties throughout its length corresponding to the mean diagram  $M(\theta)$ .

The results, with respect to ultimate strength of the test structures, are summarized in Table 3. Two different limit states were considered in defining structural "failure" — a moment (rotation capacity) criterion and a deflection criterion. The former considers failure to occur when the bending moment  $M$  reaches the random ultimate value  $M_u$  anywhere in the beam; i.e., when  $\theta$  reaches the limiting value  $\theta_u$  anywhere. Failure loads according to this criterion are indicated by heavy dots on the load-deflection graphs. Failure, according to the latter criterion, occurs when a prescribed limiting deflection,  $d_u$ , is attained. This critical deflection was taken to be the midspan deflection of the standard beam when the moment capacity limit state is reached. For the standard beam therefore, the ultimate load by either criterion is the same.



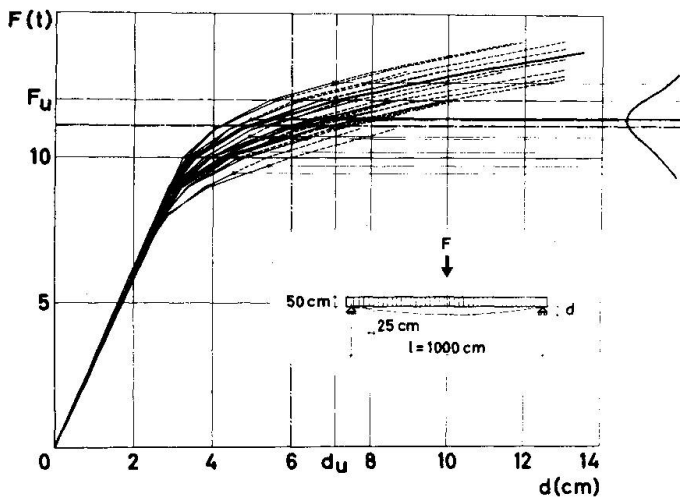


Fig. 5 — Load-deflection diagrams for structures 3.

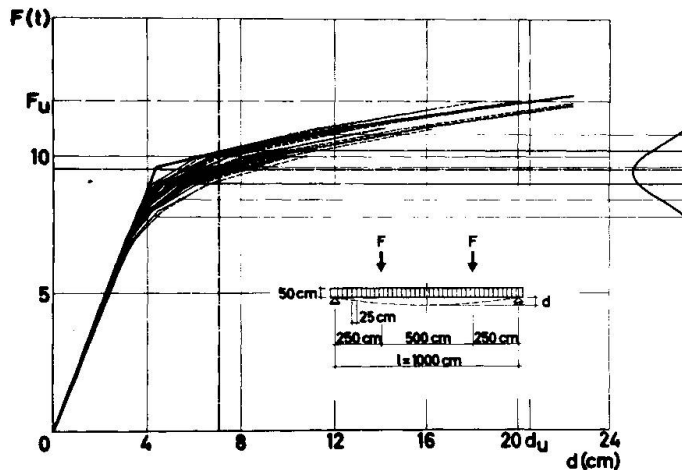


Fig. 6 — Load-deflection diagrams for structures 4.

## 6 — DISCUSSION OF TEST RESULTS

For all four structures it is obvious from the load-deflection diagrams that the mean deflection of the random beams exceeds that of the standard beam. This result is not difficult to understand in light of the skewness of the distribution  $P(\theta > \theta_i | M_i)$  previously discussed. The bias toward large values of  $\theta$  is simply carried over, through the numerical integration, as a bias toward large values of deflection. This aspect of the structural response is reflected in Table 3 by the fact that the mean ultimate strength of all structure samples, when judged by a deflection limit state, is lower than the strength of the nominal standard beam. It is also seen that the coefficients of variation of ultimate load values (3.2% - 5.3%) are significantly less than that (10%) of the original  $M_u$  values; i.e., the load-deflection diagrams exhibit considerably less dispersion than the original  $M(\theta)$  diagrams. From Table 3 it is also apparent that the reduction

in mean strength, as well as the variability of strength values, is greater for the moment capacity limit state than for the deflection criterion.

The significant difference in ultimate load probability distributions, depending on the choice of limit state, is explained by the fact that while structural deflection is influenced by material variability throughout the entire structure, moment-induced failure depends, essentially, on local material properties at a limited number of critical sections. More specifically, for the moment capacity criterion, structural strength is influenced by the following factors: the number of critical sections, the moment gradient in the vicinity of these sections, and, in the case of hyperstatic structures, the nature of the moment redistribution in the inelastic range.

The influence of these factors on mean strength may be readily discerned in the examples considered. Fig. 7 shows the bending moment distribution involved in the four test structures (based on elastic analysis for the hyperstatic cases). For isostatic structures, where moment redistribution is not a factor, the ultimate moment failure criterion corresponds essentially to a Weibull type "weakest link" theory under a prescribed stress

TABLE 3 — SUMMARY OF ULTIMATE LOAD DATA

Structure	Ult. Load Std. Beam, $F_u$ t	Moment Criterion				Deflection Criterion			
		Mean Ult. Load, t	% Reduction	Std. Dev., t	$c_v$ %	Mean Ult. Load, t	% Reduction	Std. Dev., t	$c_v$ %
		t		t	%	t		t	%
1	24	22.2	7.5	1.27	5.7	23.1	3.8	0.75	3.2
2	14.7	13.8	6.1	1.16	8.4	14.2	3.4	0.50	3.5
3	12	11.1	7.5	0.90	8.1	11.6	3.3	0.61	5.3
4	12	9.5	20.8	0.74	7.8	—	—	—	—

distribution. Regions of high uniform stress enhance failure probability, and it follows that Structure 4, with an extended region subjected to maximum bending moment (zero moment gradient), shows the most significant reduction in mean strength, 20.8%.

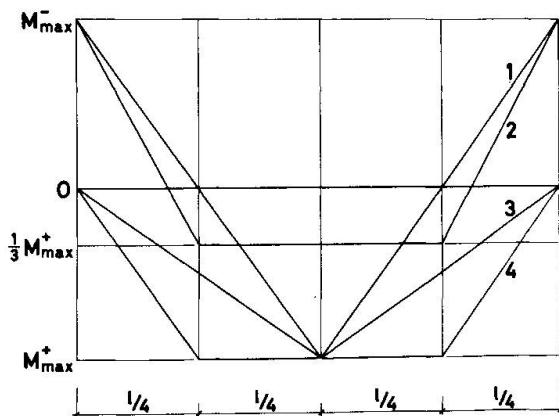


Fig. 7 — Moment gradients in test structures.

ratio,  $M_{\max}^+ / M_{\max}^- = 1$ , is maintained through the inelastic range and the randomly formed beams displayed only small variations in this ratio.

Although Structure 2 has an apparent extended critical region between the load points, moment redistribution is a significant factor in this case. For an elastically designed beam ( $M_{\max}^- = 3 M_{\max}^+$ ), redistribution in the inelastic range results in  $M_{\max}^- > 3 M_{\max}^+$ , so that only the two support sections are critical. This structure also has the steepest moment gradient in the critical regions and, consequently, it shows the smallest reduction in mean strength, 6.1%.

While these simple examples give some insight into random nonlinear behaviour, particularly with respect to mean response and general variability, the sample size is not large enough to deduce the precise nature of the response probability distribution. To obtain more significant information concerning the small failure probabilities associated with the practical range of

In comparing results for Structures 1 and 3, two opposing factors must be considered. While Structure 1 has three critical sections, against only one for Structure 3, this unfavorable factor is apparently balanced by its more favorable moment gradient, which is twice that of Structure 3. As a result, both structures show the same mean strength reduction, 7.5%. It should be noted that moment redistribution is not a significant factor in Structure 1. In fact, for the standard beam, the elastic moment

structural safety, the method can, of course, be employed with samples of larger size. Continually increasing computer capacity and speed make such an extension perfectly feasible.

## 7 - CONCLUSIONS

A computer simulation method has been presented which offers considerable promise for obtaining knowledge of the stochastic response characteristics of plane skeletal structures from a knowledge of variability in the properties of structural materials. From the results of the examples considered, the following general remarks may be made:

1. The mean strength of a population of structures is significantly less than that of a structure possessing the mean mechanical properties throughout.

2. The amount of this strength reduction depends on the moment gradient and, for statically indeterminate cases, on the nature of the moment redistribution.

3. The reduction in strength is less pronounced when failure is based on a deflection rather than a moment capacity limit state.

4. The dispersion of structural response is significantly less than that of the material properties.

The proposed method is perfectly general and may be extended to include larger samples, alternate input distributions, and more complex structures.

## REFERENCES

1. Weibull, W., "A Statistical Theory of the Strength of Materials", Ingeniörs Vetenskaps Akademien, Handlingar nr. 156, Stockholm, 1940.
2. Ferry Borges, J., "O dimensionamento de estruturas", Publicação nº.54, Laboratório Nacional de Engenharia Civil, Lisbon, 1954.
3. Ferry Borges, J., "Structural Behaviour and Safety Criteria", Preliminary Publication, VII Congress of International Association for Bridge and Structural Engineering, Rio de Janeiro, 1964.
4. Ferry Borges, J. and Arantes e Oliveira, E.R., "Non-linear Analysis of Reinforced Concrete", Publications, International Association for Bridge and Structural Engineering, Vol.23, 1963.
5. Ferry Borges, J., Arga e Lima, J., Teixeira Coelho, A., and Monteiro, V. "Analytical Results Concerning the Non-linear Behaviour of Reinforced Concrete Structures", Laboratório Nacional de Engenharia Civil, Lisbon, 1965.
6. Wold, H., "Random Normal Deviates", Tracts for Computers, No. XXV, Cambridge University Press, 1948.

## SUMMARY

The randomness of structural behaviour as influenced by the probabilistic nature of material properties is studied on basis of numerical experiments.

The numerical experiments consisted in the statistical analysis of force-displacement diagrams obtained for several simply supported and perfectly built-in beams under one or two forces. Each beam was formed by combining elements chosen at random. These elements are defined by moment-curvature diagrams belonging to a prescribed statistical population.

The examples presented give some insight on the way the statistical distributions of deflection and rupture vary in function of the types and dimensions of the structures and of the statistical distribution of the mechanical properties.

## RESUME

On étudie le caractère aléatoire du comportement des structures en tant qu'influencé par la nature probabilistique des propriétés des matériaux, prenant pour base des expériences numériques.

Les expériences numériques ont consisté dans l'analyse statistique de diagrammes forces-déplacements pour différents types de poutres, simplement appuyées et parfaitement encastrees, soumises à une ou à deux forces concentrées. Chaque poutre a été formée en combinant des éléments choisis au hasard et définis par des diagrammes moments-courbures appartenant à une population statistique.

Les exemples présentés permettent de comprendre la variation des distributions statistiques des flèches et de la rupture en fonction des types et des dimensions des structures et de la distribution statistique des propriétés mécaniques.

## ZUSAMMENFASSUNG

Die Zufälligkeit des durch die Wahrscheinlichkeitsnatur der Materialeigenschaften beeinflussten Bauwerkverhaltens ist aufgrund numerischer Experimente untersucht worden.

Die numerischen Experimente bestanden in der statistischen Auswertung der Kraft-Verschiebungs-Bilder verschiedener einfach aufgelegter und starr eingespannter Träger unter ein oder zwei Kräften. Jeder Balken war aus zu kombinierenden Elementen zufällig zusammengesetzt worden. Diesen Elementen entsprechen Moment-Krümmungs-Bilder, die zu einer bestimmten Grundgesamtheit gehören.

Die Beispiele geben einigen Einblick wie die statistische Verteilung der Durchbiegung und des Bruches in Abhängigkeit der Form, der Abmessungen und der Verteilungsfunktion der mechanischen Eigenschaften ändert.

Leere Seite  
Blank page  
Page vide

## Reliability Under Uncertain Parameters, Stochastic Loads and Resistances

Notion de sécurité, en dépit de paramètres incertains, de charges et de résistances stochastiques

Zuverlässigkeit unter Berücksichtigung unsicherer Parameter, zufälliger Lasten und Festigkeit

**K. STEVEN OTT**

Graduate Student in Structural Engineering  
Stanford University  
Stanford, California

**HARESH C. SHAH**

Associate Professor of Structural Engineering  
Stanford University  
Stanford, California

### I Description of the Problem

The feasibility of developing the mathematical tools to investigate the reliability of structural systems under probabilistic and stochastic loading is studied. The following cases are considered: 1) The reliability of systems when the probability density function of the resistance to loading is fully known, but the mean of the load distribution is a random variable governed by a probability distribution. 2) Reliability of systems subjected to narrowband, Gaussian loading when the resistance is given by a known density function. 3) The reliability of systems with constant (with respect to time), but probabilistic loads, where the resistance distribution is dependent on the load level and time.

### II Reliability of Systems with One Distribution Partially Known, the Other Fully Known

Often, it is not possible to assume that the parameters of the resistance or load distribution are fully known. In general, sampling is done in batches, i.e., a set of parameter values is obtained for each sample batch. Large differences between the various means, for example, make point estimates inaccurate. Hence, it is necessary to consider the parameters as random variables with their own density functions. In this paper only the mean will be considered as a random variable; all other parameters are assumed to be known.

Consider the case where the mean of the load is a random variable and all other parameters are known. Let

$$f_r(r_o) \sim \text{p.d.f. of the resistance}$$

$$f_l(l_o) \sim \text{p.d.f. of the load with unknown mean}$$

$$f_{\mu_1}(\mu_{1o}) \sim \text{p.d.f. of the mean of the load}$$

$$f_{r,l}(r_o, l_o) \sim \text{joint p.d.f. of load and resistance}$$

Then,

$$\rho/\mu_1 = P(r > l/\mu_1)$$

$$\rho/\mu_1 = \int_0^\infty dr_o \int_0^r dl_o \cdot f_{r,l}(r_o, l_o) = g(\mu_1) \quad (1)$$

where  $\rho$  is the reliability. The above defines the relationship between  $\rho$  and  $\mu_1$ . It is now possible to use the change of variable procedure, yielding

$$f_\rho(\rho_o) = \frac{1}{\left| \frac{\partial \rho}{\partial \mu_1} \right|} f_{\mu_1} [g^{-1}(\mu_1)] \quad (2)$$

This result will now be applied to the particular case where all distributions are Gaussian and  $r, l$  are independent, i.e.,

$$f_r(r_o) \sim N(\mu_r, \sigma_r^2)$$

$$f_{l/\mu_1}(l_o/\mu_1) \sim N(\mu_1, \sigma_1^2)$$

$$f_{\mu_1}(\mu_1) \sim N(\mu_{\mu_1}, \sigma_{\mu_1}^2)$$

$$f_x(x/\mu_1) = f_{r,l/\mu_1}(r_o, l_o/\mu_1) \sim N(\mu_r - \mu_1, \sigma_r^2 + \sigma_1^2)$$

Using eqn. 1 and 2, it can be shown that the distribution of reliability is given by,

$$f_\rho(\rho_o) = \frac{\sqrt{2\sigma_r^2 + \sigma_1^2}}{\sigma_{\mu_1}} \exp \left[ \frac{2}{\sigma_{\mu_1}^2} \left( \mu_r - \sqrt{2\sigma_r^2 + \sigma_1^2} \{ \text{erf}^{-1}(2\rho - 1) \} - \mu_{\mu_1} \right)^2 \right] \quad (3)$$

Applying equation 3 to a given problem is complicated, since it requires obtaining the inverse of an error function. It is simpler to use a numerical approach. The method recommended is perfectly general and can easily be applied to distributions other than normal. The same procedure was programmed for the computer for the case where

$$f_r(r_o) \sim N(4, \frac{1}{\sqrt{2}}), \quad f_{l/\mu_1}(\mu_1) \sim N(\mu_1, \frac{1}{\sqrt{2}}), \quad f_{\mu_1}(\mu_1) \sim N(1.5, \frac{1}{12})$$

Figure 1 shows probability distribution function for  $\rho$ . It can be seen that  $f_\rho(\rho_o)$  is skewed to the left. Furthermore, the density function approaches zero asymptotically on both sides (see Figure 1).

The sensitivity of the distribution was tested by running the computer program for various values of the parameters: 1) In Figure 2 the distribution sensitivity for  $\mu_{\mu_1}$  is shown. Note that, as  $\mu_{\mu_1}$  becomes smaller, the mean of the reliability distribution approaches 1.0 and the spread of  $f_\rho(\rho_o)$  decreases. Thus, one can conclude that the standard deviation of  $f_\rho(\rho_o)$  is quite sensitive to the mean of the  $\mu_1$  probability density function. 2) Figure 3 shows the distribution sensitivity for  $\sigma_{\mu_1}$ . The mean of  $f_\rho(\rho_o)$  is not strongly influenced by small changes in  $\sigma_{\mu_1}$ . As expected, the spread of  $f_\rho(\rho_o)$  decreases as  $\sigma_{\mu_1}$  gets smaller. 3) The distribution sensitivity for  $\sigma_1$  is shown in Figure

4 It can be seen that  $\sigma_1$  influences both the mean of  $f_\rho(\rho_o)$ ,  $\mu_\rho$ , and the



variance  $\sigma_\rho^2$ . 4) Similarly, influence of  $\sigma_r$  and  $\mu_r$  on  $f_\rho(\rho_o)$  was investigated. The effect of  $\sigma_r$  on  $f_\rho(\rho_o)$  is similar to the effect of  $\sigma_1$ . A smaller value of  $\mu_r$  is associated with a smaller  $\mu_\rho$  and a greater spread of  $f_\rho(\rho_o)$ .

### III Reliability of a Stochastically Loaded System with Probabilistic Resistance

Since the resistance is generally not known accurately, it should be considered as a random variable. Let the loading be described in the following form.  $L(t) = L_o + l(t)$  where  $L_o = \text{constant}$  and  $l(t) = \text{stochastic loading}$ . Let  $l(t)$  be narrowband, stationary, Gaussian loading with zero mean and known variance. The distribution of peaks above level  $\alpha$  is Rayleigh (ref. 2). By definition of conditional probability

$$P\{\text{reliable}\} = P\{\text{reliable load is above } \alpha\} \cdot P\{\text{load is above } \alpha\} \quad 4$$

where  $\alpha$  is any load level or

$$P\{r > l\} = P\{r > l/l > \alpha\}P\{l > \alpha\} \quad 5$$

$$\text{Let } \rho_o = P\{r > l/l = \alpha\} \quad 6$$

which will be called  $g(\alpha)$ . Note that  $\rho_o$  is a limiting value of  $\rho$ , since  $l$  cannot be exactly  $\alpha$ . Whenever  $l$  is larger than  $\alpha$ ,  $\rho$  will be smaller than  $\rho_o$ .

Using equations 4, 5 and 6 and Rayleigh distribution for peaks, the probability distribution for reliability is given by the following equation (see ref. 1).

$$f_\rho(\rho_o) = \frac{d}{d\rho_o} \left[ \rho_o \cdot \exp \left\{ \frac{(L_o - g^{-1}(\rho_o))^2}{2\sigma_y^2} \right\} \right] = \exp \left\{ \frac{L_o - g^{-1}(\rho_o)}{2\sigma_y^2} \right\} \left[ 1 - \frac{\rho_o}{2\sigma_y^2} \frac{d\{g^{-1}(\rho_o)\}}{d\rho_o} \right] \quad 7$$

Since finding  $\frac{d\{g^{-1}(\rho_o)\}}{d\rho_o}$  is complicated for most probability distributions a

numerical approach is presented here as an example. Consider an example with the following parameters

$$L_o = 0, \quad \sigma_y = \frac{1}{\sqrt{2}}, \quad f_r(r_o) \sim N(4, 1)$$

The probability density function,  $f_\rho(\rho_o)$ , is shown in Figure 5. Note that  $f_\rho(\rho_o)$  approaches a limit of  $\rho_o = 0.999968$  asymptotically. Since the Rayleigh distribution is only defined for positive values of  $\alpha$ , the reliability associated with the smallest  $\alpha$  must be the maximum  $\rho_o$ , i.e., for the numerical values given above  $(\rho_o)_{\max} = 0.999968$ . The sensitivity of the distribution was tested by running a computer program for various values of the parameters: 1) It was observed that  $f_\rho(\rho_o)$  is hardly influenced by small changes of  $\sigma_y$ . 2) Figure 6 shows the distribution sensitivity for  $L_o$ . For increasing mean load level,  $L_o$ , the reliability distribution shifts to the left. Furthermore, the maximum  $\rho_o$  becomes smaller, e.g., for  $L_o = 0.0$ ,  $(\rho_o)_{\max} = 0.999968$ ;  $L_o = 0.5$ ,  $(\rho_o)_{\max} = 0.999730$ ;  $L_o = 1.0$ ,  $(\rho_o)_{\max} = 0.998462$ . 3) The distribution sensitivity for  $\sigma_r$  is shown in Figure 7. It seems that the reliability distribution is quite strongly influenced by changes in  $\sigma_r$ . Furthermore,  $(\rho_o)_{\max}$  changes with  $\sigma_r$ , e.g., for  $\sigma_r = 0.75$ ,  $(\rho_o)_{\max} = 0.99999988$ ;  $\sigma_r = 1.00$ ,  $(\rho_o)_{\max} = 0.999968$ ;

$\sigma_r = 1.25$ ,  $(\rho_o)_{\max} = 0.999233$ . 4) The influence of  $\mu_r$  on  $f_\rho(\rho_o)$  is shown in Figure 8. As expected  $(\rho_o)_{\max}$  is affected by  $\mu_r$ , e.g.,  $\mu_r = 3.50$ ,  $(\rho_o)_{\max} = 0.999730$ ;  $\mu_r = 4.00$ ,  $(\rho_o)_{\max} = 0.999968$ .

#### IV Reliability of Systems with Stochastic, Load Dependent Resistance

Structural systems subjected to loads will generally experience a deterioration of strength with time due to such physical phenomena as creep, metal fatigue, etc. The rate of loss of strength often depends on the load level, e.g., a reinforced concrete beam will usually experience a greater rate of creep if it is subjected to a larger load than if it is subjected to a smaller load. Consider a model whose behavior is: a) Loads are random, but not time varying. b) The only parameter of the resistance distribution, which is load and time dependent, is the mean,  $\mu_r(r, t, \ell)$ . c) A family of functions exists completely defining the change of the mean  $\mu_r$  with respect to time and load. Condition (c) stated above is shown in Figure 9. Given a load  $\ell_1$  and time  $t_1$ , it is possible to find the mean of the resistance which in turn defines the probability density function of the resistance. Let  $f_\ell(\ell_o) \sim$  p.d.f of the load,  $\mu_r = g(\ell, t)$ ,  $f_{r/\mu_r}(r_o/\mu_r) \sim$  p.d.f of the resistance given the mean. Consider a particular time,  $t_o$ . The random variable  $\mu_r$  at time,  $t_o$  is only a function of the random variable  $\ell$ . It is possible to find  $f_{\mu_r}$  by using the change of variable procedure.

$$f_{\mu_r}(\mu_r) = \frac{1}{\left| \frac{\partial g(\mu_r)}{\partial \ell} \right|} f_\ell\{g^{-1}(\ell)\}$$

Following the same procedure discussed in previous section one obtains

$$f_\rho(\rho_o/t) = \frac{1}{\left| \frac{\partial \rho}{\partial \mu_r} \right|} f_{\mu_r}\{g^{-1}(\mu_r)\} \quad 8$$

where  $\rho/\mu_r = g(\mu_r) = \int_0^\infty dr_o \int_0^r d\ell_o f_{r,\ell}(r_o, \ell_o)$ .

This result will now be applied to the particular case where both the resistance and load distributions are normal and the mean is related to the load and time by a linear function, i.e.,

$$\begin{aligned} 1) \quad f_\ell(\ell_o) &\sim N(\mu_\ell, \sigma_\ell^2) & 2) \quad \mu_r &= - (m\ell + b)t + c = g(\ell, t) \\ 3) \quad f_{r/\mu_r}(r_o/\mu_r) &\sim N(\mu_r, \sigma_r^2) \end{aligned} \quad 9$$

$$\text{Then, } \rho = P(r > \ell/\mu_r) = P(r - \ell > 0/\mu_r) = \frac{1}{\sqrt{2\pi(\sigma_r^2/\sigma_r^2 + \sigma_\ell^2)}} \int_0^\infty \exp\left[-\frac{\{x - (\mu_r - \mu_\ell)\}^2}{2(\sigma_r^2/\sigma_r^2 + \sigma_\ell^2)}\right] dx$$

Following similar procedure as mentioned in previous sections, it can be shown that

$$\begin{aligned} f_{\rho/t}(\rho_o/t) &= \frac{\sqrt{\sigma_r^2 + \sigma_\ell^2}}{mt \cdot \sigma_\ell} \cdot \\ &\cdot \exp\left[\frac{1}{2(\sigma_\ell mt)^2} \left\{ \mu_\ell \sqrt{\sigma_r^2 + \sigma_\ell^2} [\text{erf}^{-1}(2\rho - 1)] - c + t[b - m\mu_\ell] \right\}^2\right] \end{aligned} \quad 10$$

This equation cannot be used directly, since it involves the inverse of the error function. Hence, it is necessary to develop a numerical method. Consider the following numerical example

$$f_{\ell}(\ell_0) \sim N(5.1) , \quad \mu_r = -0.5 \cdot t \cdot \ell + 10.0 , \quad f_{r/\mu_r}(r_0/\mu_r) \sim N(\mu_r, 1) \quad (11)$$

The results of the computation are shown in Figure 10. At  $T = 0$  the reliability distribution is asymptotic to  $\rho = 1$  with half of the probability mass concentrated between  $\rho = 0.99999921$  and  $\rho = 1.0$ . At  $T = 2$  the reliability function is symmetric about  $\rho = 0.5$  and asymptotic to both zero and one. At  $T = 4$  there is a probability of 0.5 that  $\rho$  will lie between 0.0 and 0.000005413. Thus, it can be seen that the probability mass shifts from a reliability close to 1.0 to a reliability close to 0.0 with the passage of time. Since  $\rho$  is a function of time,  $f_{\rho}(\rho_0)$  is also time dependent. In Figure 11  $f_{\rho}(\rho_0)$  vs. time is shown. Prior to  $t = 1$  most of the probability mass is concentrated between  $\rho = 0.99$  and  $\rho = 1.00$ . Close to time period 1 the probability mass moves through the point  $\rho = 0.99$ . During the subsequent time periods the probability of  $\rho$  being 0.99 decreases. The sensitivity of the distributions was tested by running a computer program for various values of the parameters and three different time periods ( $t = 0.0$ ,  $t = 1.5$ ,  $t = 3.0$ ; circled numbers on subsequent graphs indicate the corresponding reliability distribution). 1) In Figure 12 the distribution sensitivity for  $\mu_{\ell}$  is shown. As  $\mu_{\ell}$  becomes larger, the probability mass shifts from a high to a low reliability more rapidly. Furthermore, for larger values of  $\mu_{\ell}$  the asymptote  $\rho = 1.0$  is approached faster. 2) Figure 13 shows the distribution sensitivity for  $\sigma_{\ell}$ . Except for higher peaks corresponding to lower values of  $\sigma_{\ell}$  (Figure 13) small changes of this parameter do not influence  $f_{\rho}(\rho_0)$  significantly. 3) The distribution sensitivity for  $\sigma_r$  is shown in Figure 14. Similarly to  $\sigma_{\ell}$ ,  $\sigma_r$  hardly influences the reliability distribution. Note that in this case the peaks are higher for larger values of  $\sigma_r$ . 4) The influence of the slope,  $m$ , on the reliability distribution is shown in Figure 15. Small changes in  $m$  cause fairly large changes in  $f_{\rho}(\rho_0)$ . As the slope decreases, the shifting of probability mass from a high reliability to a low reliability takes place more rapidly, i.e. a system has a greater probability of survival over time if the slope is large. 5) The influence of the intercept,  $c$ , shown in Figure 16 is quite pronounced. For large values of  $c$  the shifting of probability mass takes place at a later time period.

## V Conclusions

As was shown, the derivations of the reliability distributions is fairly simple for the case where only one parameter is a random variable. However, even in this case it is not possible to find a usable, analytical solution for the distributions chosen. Further work needs to be done in trying to develop simple closed form solutions — possibly using approximations or investigating various distributions. It would be interesting to see this idea expanded to the case where not only the mean, but also the variance is random.

## References:

1. Reliability under Uncertain Parameters, Stochastic Loads and Resistances, K. Steven Ott, Engineer's Thesis, Stanford 1969.
2. Random Vibrations, Crandall and Mark, Academic Press, 1963.
3. Probability, Random Variables, and Stochastic Processes, A. Papoulis, McGraw-Hill, New York, 1965.

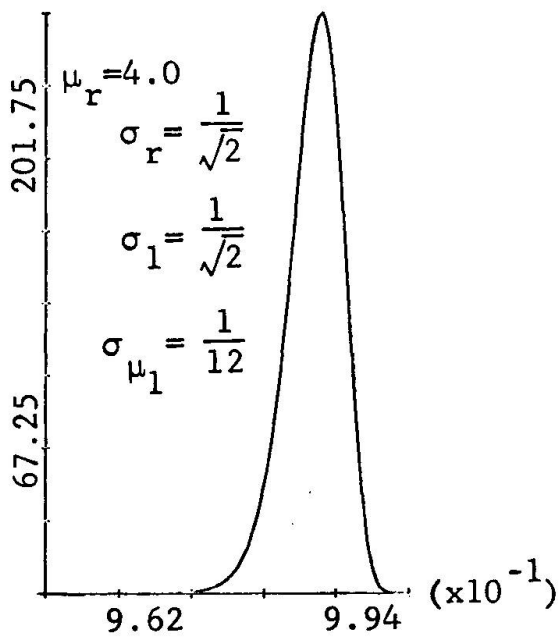


FIG. 1

Distribution Sensitivity

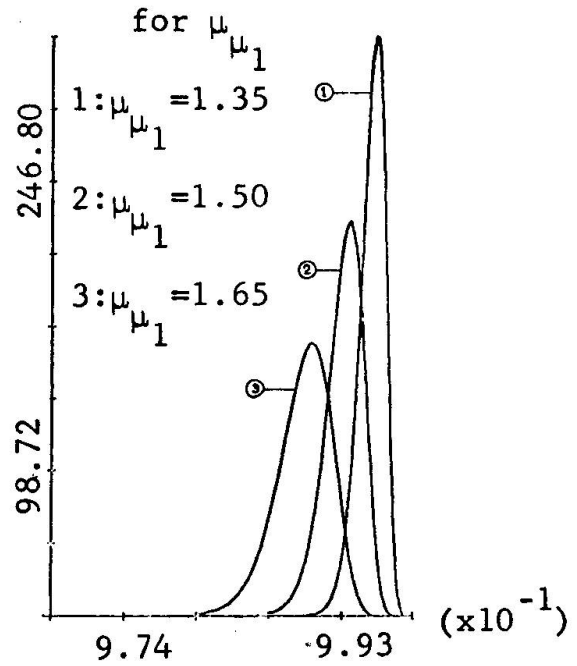


FIG. 2

Distribution Sensitivity

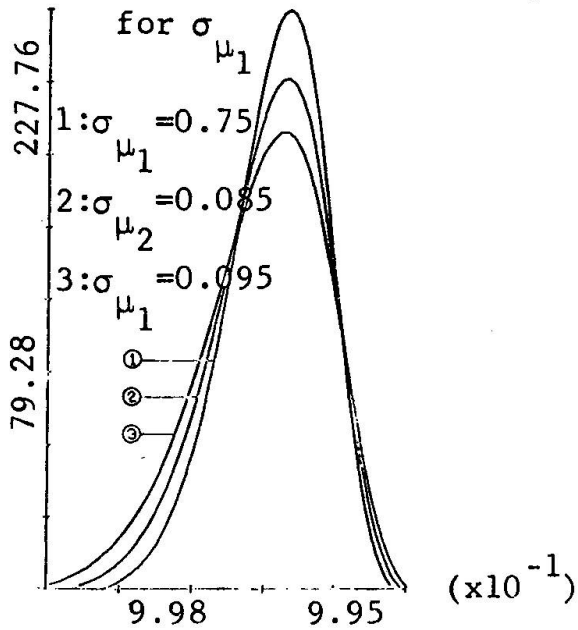


FIG. 3

Distribution Sensitivity for  $\sigma_1$

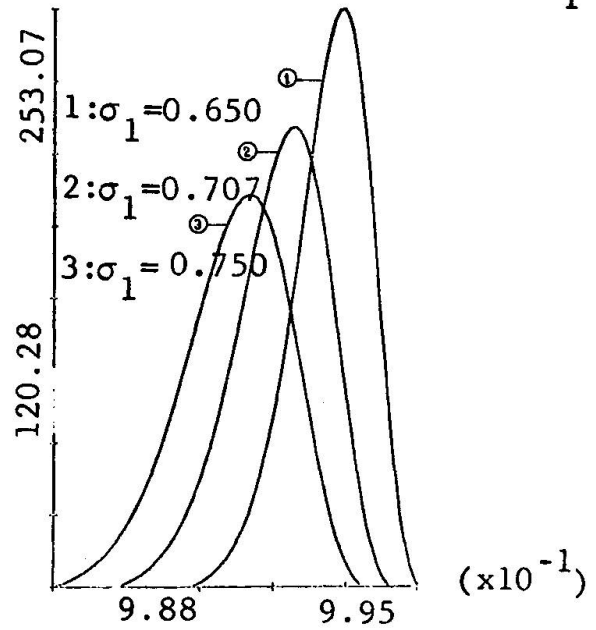


FIG. 4

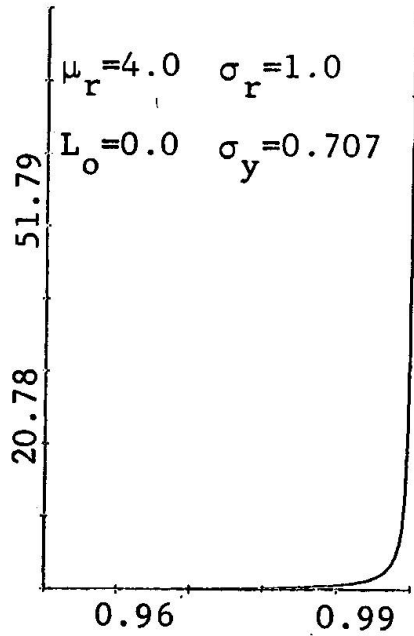


FIG. 5

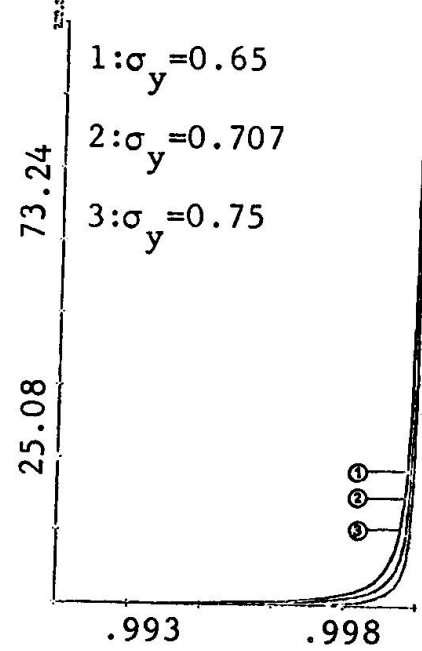
Distribution Sensitivity for  $\sigma_y$ 

FIG. 6

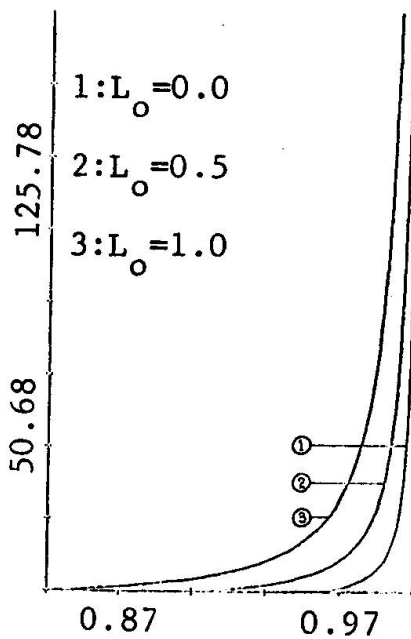
Distribution Sensitivity for  $L_o$ 

FIG. 7

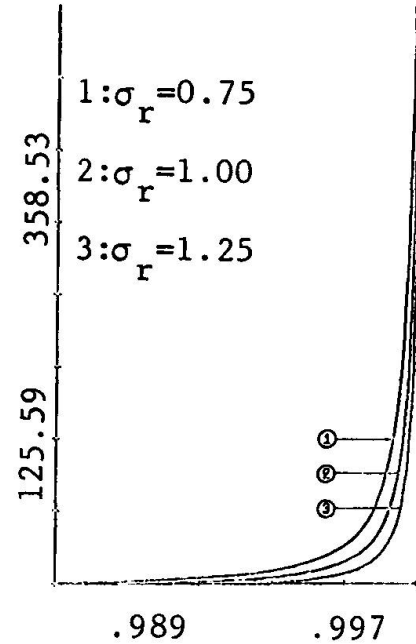
Distribution Sensitivity for  $\sigma_r$ 

FIG. 8

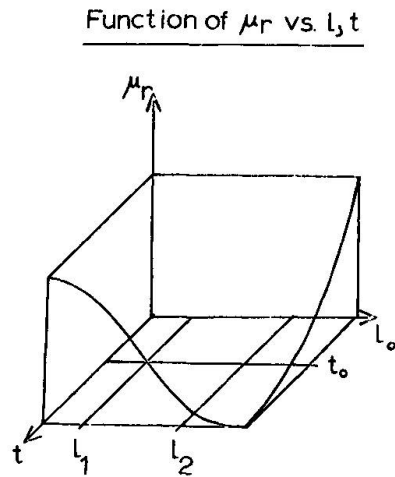


Figure 9

Reliability Distributions

$\mu_t = 5.00$   $\sigma_t = 100$   
 $\sigma_r = 100$   
 Slope = -0.5 Intercept = 100

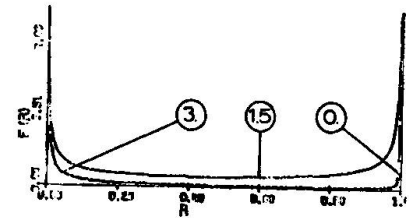


Figure 10

Density vs. Time for Constant  $\rho$

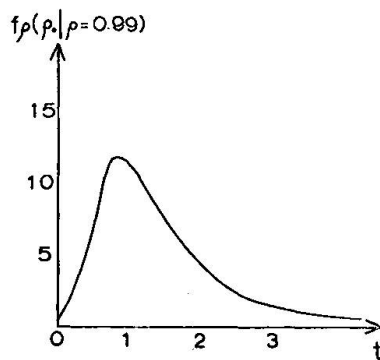


Figure 11

Distribution Sensitivity

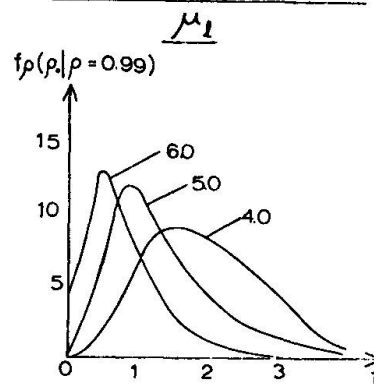


Figure 12

Distribution Sensitivity

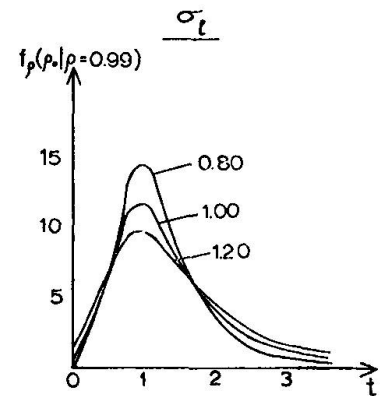


Figure 13

Distribution Sensitivity

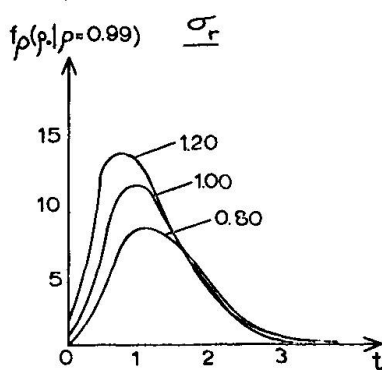


Figure 14

Distribution Sensitivity

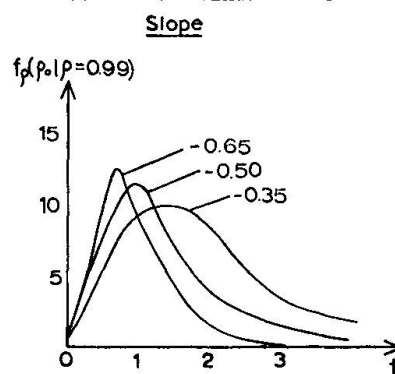


Figure 15

Distribution Sensitivity

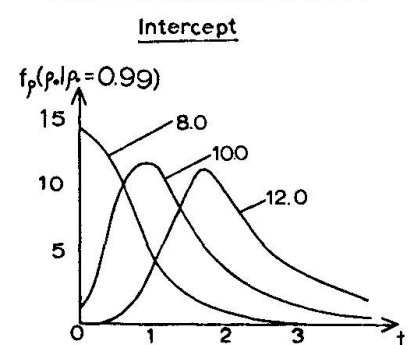


Figure 16